Spherical Perspective

António B. Araújo

Abstract We survey the present state of spherical perspective, regarding both mathematical structure and drawing practice, with a view to applications in the visual arts. We define a spherical perspective as the entailment of a conical anamorphosis with a compact flattening of the visual sphere. We examine a general framework for solving spherical perspectives, exemplified with the azimuthal equidistant ("fisheye") and equirectangular cases. We consider the relation between spherical and curvilinear perspectives. We briefly discuss computer renderings, but focus on methods adapted to freehand sketching or technical drawing with simple instruments such as ruler and compass. We discuss how handmade spherical perspective drawings can generate immersive anamorphoses, which can be rendered as virtual reality panoramas, leading to hybrid visual creations that bridge the gap between traditional drawing and digital environments.

Keywords

Spherical perspective, anamorphosis, fisheye, equirectangular, drawing, curvilinear perspective, virtual reality panoramas

Preprint Notice

This is a pre-print version of a chapter published in the Handbook of the Mathematics of the Arts and Sciences. The final authenticated version is available online at https://doi.org/10.1007/978-3-319-70658-0_100-1

António B. Araújo
CIAC-UAb, Center for Research in Arts and Communication, Universidade Aberta, R. Escola Politécnica, 141-147, 1269-001, Lisbon, Portugal e-mail: antonio.araujo@uab.pt

The final version differs in page and image numbering and has other minor changes. Please cite the published work as

A. B. Araújo, "Spherical Perspective," in Handbook of the Mathematics of the Arts and Sciences, B. Sriraman, Ed. Cham: Springer International Publishing, 2021, pp. 1–61. https://doi.org/10.1007/978-3-319-70658-0_100-1

Introduction

We will survey ahead the present state of spherical perspective, discuss its mathematical definition and its connection to immersive visualizations and anamorphoses. We are interested in spherical perspective both as a mathematical object and as a practical discipline of drawing, that connects traditional technical drawing with digital visualization methods.

We start by briefly discussing the history of spherical perspectives and then redefining them, taking anamorphosis as the central concept. Then we consider how to solve the two perspectives that we have chosen as main examples: the azimuthal equidistant ("fisheye") and equirectangular cases. From the parallels found between the solutions obtained, we infer a general framework for approaching arbitrary cases.

In the present work we are interested in a notion of perspective that can be both mathematically rigorous and executable by the human hand, not requiring modern digital machinery. Such drawing has a long history of fertile interactions between mathematics and art, a tradition of *rational drawing* (Araújo 2020) that straddles mathematics and art, connecting the hand, the eye, and the mind. It is an intellectual thread that we can trace at least back to Euclid (through both his Optics (Brownson 1981) and his Geometry), and touches and endless multitude of artists, engineers, architects, some of them sound theoreticians, most of them delightful and sometimes infuriating hackers, and once in a while brushes again against a mathematician proper, often a now surprising name, such as Taylor - yes, that Taylor (Andersen 1992), mostly now known by his series rather than by his views on vanishing points.

This thread of rational drawing also connects strongly with modern ideas of graphical computing, but we are mostly concerned with what new drawing software can be installed in our minds and hands. Computers will be mostly considered as means of displaying such constructions. This should not be read - quite the opposite - as any deprecation of the shining role of computer graphics in the both geometric investigation and artistic creation in the area of immersive drawing, but rather as an attempt to focus on one other domain, sometimes lost in that bright light, and which has its own scope and enduring interest that is deserving of consideration, especially for those of us who see handmade drawing not only as a means of expression but as a mode of thought.

History

Spherical perpective had a curious development, with many false starts and equivocations. It can be argued that the first spherical perspective was not spherical and the next spherical perspectives were not perspectives.

The first was 's formal treatment of the azimuthal equidistant spherical perspective (commonly called *fisheye* perspective) in their 1968 book *La Perspective Curviligne* Barre and Flocon (1968, 1987). This was a proper perspective, in the sense that it provided a system to calculate and render all points, lines, planes, and vanishing points, using only ruler and compass constructions, to an approximation with controlled error bounds. Yet *spherical* perspective is somewhat of a misnomer, as those same rules were only set for half of the sphere, rendering therefore only a 180-degree view around a central axis, in what is often called, in a rather ambiguous way, a .

Later attempts at spherical perspectives suffered from the opposite problem: they were fully spherical (so-called), but they weren't actually *perspectives* by the standards set up by Barre and Flocon (or indeed by classical perspective), i.e., they were not general, rigorous methods for calculating all vanishing points and line images. They were either qualitative, ad-hoc, or partial, grid-based methods. Later, they were computer-based (see for instance Correia et al (2013)), moving out of the reach of the human draughtsman; some problems are dropped rather than solved.

In a *Leonardo* paper, Casas (1983) writes of a setup that seems at first sight a generalization of (Barre and Flocon 1968) (though not claiming to be so and in fact never citing their work - it is unclear if Casas was familiar with it), but is limited to qualitative observations that apply both to such a generalization and to a whole class of so-called 6-point perspectives. Further, these qualitative observations suffer from peculiar misconceptions regarding the behaviour of the projection near what we here will call its blowup, that is, the point at which the projection from the sphere to the plane is not defined . For instance, Casas states that the sphere flattening cannot be achieved mathematically but only *graphically*. What is meant by this is somewhat cryptic; Casas difficulties seem to be at times related to the topological differences between the sphere and the projection disc, sometimes to the well-known fact that the plane and sphere are not isometric, sometimes to a misconception that lines going to the blow-up point should widen to non-zero measure regions as they approach it. The author was apparently unaware, unlike Flocon, Barre and Bouligand in their discussion of the theoretical aspects of their perspective (Barre et al 1964) that the flattening itself is not new. It is the azimuthal equidistant projection, well known in cartography. The real question is how to calculate it in a way appropriate for drawing with simple instruments and how to relate the projection to the spatial scene in an elegant way. This is alluded to by K. R. Adams in a letter to Leonardo (Adams 1983). Adams was the author of another spherical perspective (Adams 1976), the (based on a flattening of a tetrahedron), and was aware of the real problem: of balancing the pros and cons of various projections, their topological and metric properties, and the possibility of plotting them efficiently by simple means such as ruler and compass.

Casas provides no specific metric description of his projection, being seemingly convinced of the impossibility of doing so; He would later publish a second paper in Leonardo (Casas 1984), describing a spherical picture-whithin-picture recursive graphical device reminiscent of the so-called Droste effect in Escher's *Print Gallery* (Escher 1956) (de Smit and Lenstra Jr 2003), again worked qualitatively.

Moose (1986), in an attempt to make specific and practical the qualitative considerations of Casas, proposed a with an angle of view wider than 180 degrees and, with a specific construction in ruler and compass. It is, however, a rather ad-hoc construction, and not a generalization of Barre and Flocon's.

approaches the problem in a clear and pragmatic fashion, understanding correctly that the azimuthal equidistant projection can be extended all the way to a 360 degrees view (Michel 2013). Michel constructs a correct grid of horizontal and vertical line projections on which measurements from observation can be plotted and lines drawn by interpolation on the grid. This does not constitute a formal "perspective" in the sense that Barre and Flocon's work does; rather, it is a , but unlike Casas it is well defined and unlike Moose's it is indeed a generalization of Barre and Flocon's to a 360-degree view. This informal scheme, in the hands of a virtuoso draughtsman like G. Michel, is quite enough to produce exquisite drawings in 360 degree spherical perspective. A much similar gridding method was applied by the same author to the equirectangular case (Michel n.d.). In a private communication, the present author was informed by G. Michel that his approach was made independently of Barre and Flocon's. In fact, a main instrument of these authors - the approximation of lines by arcs of circle in the anterior hemisphere (as we will see ahead) is absent from Michel's work, who works from exact azimuthal equidistant grids, through freehand interpolation, without explicit consideration of error bounds.

In contrast to these works, A. B. Araújo Araújo (2018c) proposes a formal perspective in the sense of Barre and Flocon, meaning a systematic method to obtain all line images and their vanishing points for any given 3D scene, with consideration of formal ruler and compass interpolations. This perspective is the total azimuthal equidistant spherical perspective, that is, the formal generalization of Barre and Flocon's "fisheye" perspective to the full sphere. This is the main work we will be describing and developing here, so let us consider its main points in a quick summary.

The work can be divided in two parts: 1) a general definition of spherical perspectives and a framework for their study and 2) the application of this framework to the azimuthal equidistant case.

A spherical perspective is defined as a two-step process: a spherical anamorphosis followed by a cartographic flattening.

Anamorphosis itself is redefined as an equivalence relation between three dimensional sets, each three-dimensional scene being represented by a canonical anamorphic image on the surface of a sphere. This concept of anamorphosis has been studied at length in another chapter in the present volume (see chapter Anamorphosis Reformed: from Optical Illusions to Immersive Perspectives) but we will recall it ahead briefly. The main point is that the canonical anamorphosis is the same for any spherical perspective, and it is very symmetrical; each spatial line is represented as a (half of a geodesic) ending at exactly two vanishing points to each other. These

vanishing points are functions of the observation point and of the lines themselves, not depending on the projection chosen for a particular perspective.

In the second step, this anamorphic image is projected onto a compact subset of the plane by a flattening map, which is usually a cartographic map of the sphere. The resulting picture, flat and bounded, is what we call the perspective drawing. Implicit here is also a philosophy of *compactness* - that is, unlike classical perspective, the spherical perspective picture, including is vanishing points should be fully contained in a prescribed bounded and closed region of the plane where the drawing is to be performed. In fact, ideally, even the auxiliary construction diagrams should be fully contained therein.

This approach separates the mimetic from the representational aspects of the problem and suggests a general approach to solving a spherical perspective. Unlike the previous approaches above, the focus shifts from lines to geodesics (the vanishing sets of spatial planes) and an emphasis is placed on the importance of vanishing points always arising as .

Each perspective is characterized by the particular form of its flattening map, and this naturally breaks up the set of geodesics into classes which must be handled differently to get an efficient rendering of the perspective. This partition and its rendering methods turn out to rely heavily on the duality of vanishing points. Beyond the original azimuthal equidistant case treated in Araújo (2018c), this approach was also fruitful in the equirectangular (Araújo 2018b) and cubical (Araújo et al 2020) cases. These latter cases relate naturally to VR visualizations, using the perspective drawings as data sources for VR panoramas. This establishes an interesting connection between the development of hand drawn perspectives and immersive computer graphics, at both a theoretical and artistic level (Araújo et al 2019; Olivero et al 2019b). Spherical perspective had become somewhat split after Flocon and Barre, with handmade practice being handled mostly by gridding or had-hoc sketching with little new mathematical insight, and most new developments taking place at the computational level in ways that required computers to render a scene (see for instance the software of Correia et al (2013) which can render a scene in parametric curvilinear perspectives). The methods we will present ahead are focused on understanding spherical perspective in a theoretically meaningful way, and rendering it in a way that is appropriate for hand drawing, yet accurate enough to serve as a basis for the creation of immersive VR visualizations.

Spherical anamorphosis

To understand spherical perspective we need to review spherical anamorphosis. We will first approach the subject loosely, and then restate it formally.

Radial occlusion and mimesis

Suppose you are stuck to a point in space but free to look around you in any direction. You want to make a drawing that captures all that you see. How would you go about it?

The question is too open ended. This really depends on what you are allowed to draw, and how. It also depends on what "capturing what you see means". Ultimately, we will want to define a spherical perspective as a drawing done on a bounded and closed region of the plane, which represents all the visual data accessible from a fixed observation point. But before we get to that definition we will relax one of those criteria. If we are allowed to draw on a curved surface, we can give a very precise meaning to the notion of "capturing what we see".

The answer lies in . This is a word used to denote several different concepts. Here we mean it in a way that follows more in line with Euclid's optics (Burton (1945), Brownson (1981)) than with its usual definition derived from linear perspective. The reader may find a careful accounting of this notion in the chapter Anamorphosis Reformed: from Optical Illusions to Immersive Perspectives in the present volume, or in Araújo (2017, 2018c). Here we will proceed loosely:

It is an empirical fact that under certain optical setups, two points will "look the same" (i.e., seem to occupy the same position in the visual field) for an observer at a point O if and only if they lie on the same ray from O. More generally, two 3D objects will "look the same" (i.e., seem to occupy the same region of the visual field) if and only if the set of their points define the same cone of rays from O. This is an empirical fact that we call the principle of : visual occlusion coincides with geometrical alignment. This is not a mathematical truth, but a geometric statement of an empirical fact that is only verified when special circumstances (optical media, lighting conditions, geometric conditions) are themselves verified. It fails whenever refraction or reflection effects are strong enough, for instance, or when for some reason or another the abstraction of a monocular observer stationed at a point is not adequate. We will not be concerned with specifying all those conditions, but simply in deriving the interesting conclusions that result when the principle is indeed verified.

For instance, if two objects look the same from O whenever they have the same cone of rays from O, it follows that every 3D object X has an infinity of other objects that look exactly like it from point O. We will call these objects the of X relative to O (the O-anamorphs of X, for short). This defines an equivalence relation between objects. It also follows that there are anamorphs of X which are two-dimensional, since, if you intersect the cone of rays of X with an adequate surface S, the intersection will be a two-dimensional object and by construction will have the same cone of rays as X. We call the closure of this 2D projection, uniquely defined by O, S, X, the anamorphosis of X onto S relative to O.

Since the space of rays from O is itself isomorphic to the unit sphere around O, this sphere is the most natural choice of projection surface to define anamorphosis relative to O. It records every ray in the most symmetrical way possible, and every other surface anamorphosis can be obtained from it, so that it can be called the

canonical anamorphosis. Further, it ”captures” this information in a very concrete sense: if the principle of radial occlusion is assumed, then the anamorphosis results in : an observer standing at O and looking at the anamorphic drawing on the sphere would be unable to distinguish the anamorphic drawing on the sphere from the actual 3D environment from which the drawing was obtained. For instance, in Figure 1, if the 3D cube were to be replaced by its conical projection on the sphere, the observer at the center of the sphere would not notice the switch.

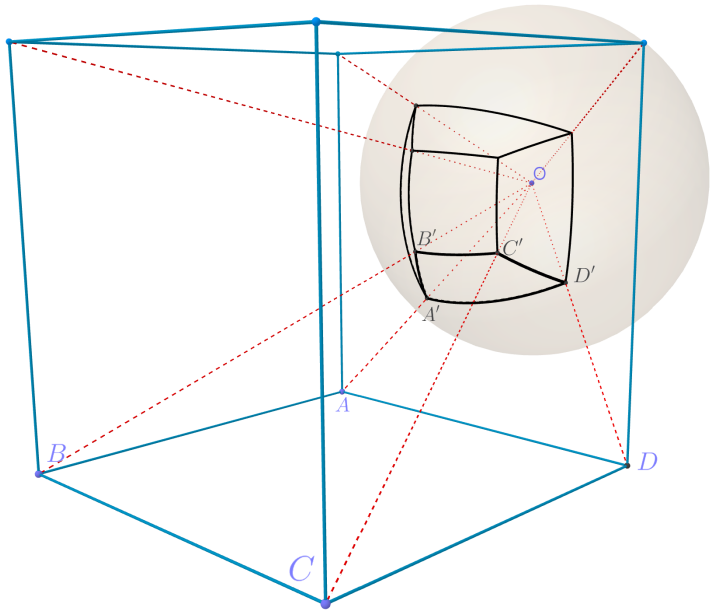

Fig. 1 Anamorph of a cube on a sphere. The 3D cube is projected radially towards O to obtain a 2D anamorph on the surface of the sphere. The 2D anamorph would look exactly like the 3D object for an observer at O, if the principle of visual occlusion is valid.

This projection onto the sphere, although it has the same visual information as the 3D scene (when seen from O), has very different and interesting properties. Unlike the original scene, the anamorphic image is bounded, as the sphere is compact. And if we make it compact (bounded and closed) this gives rise to a natural notion of vanishing points. Let us explore this in the next section, while making the concept rigorous.

Note 1. The notions of and are often conflated in the literature, and are not at all standard. For instance, Catalano (1986) calls spherical perspective to what we here call spherical anamorphosis. , who is famous for his spherical paintings (which are spherical anamorphoses by our definition) uses a mix of the two terms, for instance Termes (1991) calls 5-point spherical perspective to the hemispherical perspective of Barre and Flocon (fisheye perspective), but calls six-point perspective to what we

define here as spherical anamorphosis. Termes uses two separate, complementary fisheye perspectives to arrange on the plane the projection of a full sphere anamorphosis (Termes 1998, 1991), which technically counts as a total spherical perspective as we will define the term ahead. It can be argued that the conflation of the terms perspective and anamorphosis has led to much confusion historically (see chapter Anamorphosis Reformed: from Optical Illusions to Immersive Perspectives or (Araújo 2016)) and in the present work we use the term spherical *perspective* exclusively for a representation on the plane (that follows certain conditions explained ahead) and never for the anamorphic drawing on the sphere.

Spherical anamorphs and their vanishing points

Let us formalize the intuitions of the previous section. We have seen that accepting the principle of radial occlusion means that all the visual information of a scene, relative to an observation point, is held by the visual cone of the scene.

By an *observer* we mean a point O in three-dimensional Euclidean space. Let $\mathscr{R}_O$ be the set of rays from O. Let S^2_O be the unit sphere centered at O. The map $P \mapsto \overrightarrow{OP}$ is a bijection between the sphere of center O and the set of rays from O, identifying each ray from O with the point where the ray crosses the sphere. Hence we can speak of from O and points on the sphere S^2_O interchangeably.

Definition 1. Given a set Σ we say that $C_O(\Sigma) = \{\overrightarrow{OP} : P \in \Sigma\}$ is the *of Σ relative to O. The of Σ onto S^2_O is the the intersection of the visual cone with the unit sphere, $C_O(\Sigma) \cap S^2_O$. We identify freely the cone with the conical projection on the sphere whenever context is clear.*

We will have a special interest in sets like planes and lines, so the following example is vital:

Example 1. Visual cone of a line: Consider a line l not containing O. The visual cone of l relative to O is a half-plane minus a line. For, let H_l be the single plane that contains both O and l. Let l_O be the translation of l to O, which is parallel to l. Then the rays from O to points of l cover the half-plane of H_l that contains l and is bounded by l_O , with the exception of l_O itself. $l_O \setminus \{O\}$ is the union of two diametrically opposite rays $V, V^\star$. These are not in the cone since they are parallel to l and therefore do not intersect it. Intuitively, the eye, following along the length of l to infinity (in both directions) approaches but never reaches these two diametrically opposite limit directions.

Now consider the conical image of the visual cone on the sphere, $C_O(\Sigma) \cap S^2_O$ (see Figure 2). Plane H_l intersects the sphere in a geodesic of the sphere, and the visual cone $C_O(l)$ projects on half that geodesic, that is, on a *meridian* of the sphere. The meridian will be missing it's two endpoints V and $V^\star$, corresponding to the two rays that make up $l_O \setminus \{O\}$.

We recall that a of the sphere is a on the sphere, that is, a circle with the same radius as the sphere itself. A geodesic is defined by intersecting the sphere with a plane passing through O.

So we see that the visual cone of a line is a missing two rays, or, equivalently, on the sphere it is a meridian missing its two endpoints. Now, we rather dislike that these points are missing, and we will do something about that. But first we must recall some topological notions.

Definition 2. Let S be a subset of a topological space. We say that P is a of S if every neighbourhood of P, no matter how small, contains a point Q of S other than P. The of S is the union of S with its limit points, and is denoted by $cl(S)$. We say S is if $S = cl(S)$. The of S is the closure of S minus the set itself, denoted $Res(S) = cl(S) \setminus S$.

Intuitively: a limit point of a set is a point you can approach as close as you want without leaving the set. Closed sets are those that contain all their limit points. For instance, spatial points, lines and planes are closed. A line segment with its endpoints included is closed. But a line segment without its endpoints is not closed, as its missing endpoints are limit points of the set. We are interested in these notions because they will relate to the notion of vanishing points ahead. We are now ready to proceed:

We call *objects* to closed sets in three-dimensional space. A *scene* is a finite set of objects.

There is on $\mathscr{R}_O$ a single topology that makes the from S^2_O to $\mathscr{R}_O$ continuous both ways (a). We will from now on endow the set of rays with this topology, so we can speak of the topological closure of a set of rays from O.

In topological terms, we saw in example 1 that a spatial line - which is closed but unbounded - has a visual cone (the meridian on the sphere) which is *bounded*. However, it is not closed, since it is missing its endpoints.

We call *compact* set to a set that is both closed and bounded.

Now, speaking intuitively, sets are all that we can draw. We cannot draw an infinite line, only a bounded one. And we cannot really draw a line missing endpoints. Things going to infinity or things missing endpoints, are things that we can signify but not really draw. The point of anamorphosis is to replace the real 3D object - closed but unbounded by another - its spherical anamorph - that is visually equivalent to it, and yet is compact, hence drawable.

To achieve that, we cannot simply take the strict conical projection, since as we have seen it will not contain the endpoints of a line image. These two missing endpoints of the meridian, correspond naturally to the notion of vanishing points. We add them to conical projection by taking the topological closure and call the resulting compact object a *spherical anamorphosis*. This is the visual equivalent of the original 3D object, but is 2D, bounded, and closed: a *drawing*, even if one made on a curved surface.

Definition 3. Let Σ be a scene. We say that $\Lambda_O(\Sigma) = cl(C_O(\Sigma) \cap S^2_O)$ is the of Σ relative to O. Let $\lambda_O : \mathbb{R}^3 \setminus \{O\} \to S^2_O$ be the map $P \mapsto \overrightarrow{OP} \cap S^2_O$. We call λ_O the

anamorphism (or conical projection) onto S^2_O relative to O. We use the same name for the corresponding map $\lambda_O : \mathscr{R}_O \to S^2_O$. We have $\Lambda_O(\Sigma) = cl(\lambda_O(\Sigma))$.

Definition 4. We say that $\mathscr{V}_O(\Sigma) = cl(C_O(\Sigma)) \setminus C_O(\Sigma)$ is the set of of scene Σ relative to O. We say that $\mathscr{V}_O(\Sigma) \cap S^2_O$ is the set of vanishing points of Σ in the spherical anamorphosis $\Lambda_O(\Sigma)$.

So, we define the anamorphosis of a scene onto the sphere to be the topological closure of the strict conical projection. That is, the anamorphosis is what we get if we add the missing limit points to the strict conical projection. And to those missing points we have to add to make the anamorphosis closed we call the vanishing points.

Note 2. Note that both the anamorphosis and the vanishing points of a scene are naturally defined on the space of rays, and depend only on the scene and on the viewpoint. Of course rays and points on the sphere are the same thing. When we view the anamorphosis on the sphere we can think more concretely, using the sphere as a projection surface. In Araújo (2018c), or in the present volume's chapter Anamorphosis Reformed: from Optical Illusions to Immersive Perspectives anamorphosis is defined for more general surfaces, but the spherical anamorphosis is the canonical one, from which all others can be derived (again because the sphere is identified with the space of rays) and since we are only interested in spherical perspectives here, we will discard further generality.

From example 1 we see that the vanishing points of a line l are obtained by translating the line to O and intersecting it with the sphere. Since parallel lines will have the same translated line at O, their vanishing points are equal. Hence vanishing points of lines are *meeting* points for their anamorphic images, thus preserving the main feature of the classical notion of vanishing points.

We note that the vanishing points of a line are to each other. Recall that given a point P on a sphere, the of a point P is the point to P on the sphere. From now on we denote the antipode of a point P by $P^\star$.

Proposition 1. *The spherical anamorphosis of a line l not containing O is a meridian ending at two antipodal vanishing points, given by $l_O \cap S^2_O$, where l_O is the translation of l to O. Hence have the same vanishing points.*

See for instance in Figure 2 the two parallel lines l and j. Their planes H_l and H_j intersect at the common parallel line through O, which in turn projects onto the sphere at two antipodal points V and $V^\star$, which are for the which are the anamorphic images of the spatial lines.

Along with lines and points, planes are the most important objects in perspective. Their projections are very simple:

Proposition 2. *Let σ be a plane that does not contain O. Let σ_O be the translation of σ to O. The intersection of σ_O with the sphere is a geodesic, which is the vanishing set $\mathscr{V}_O(\sigma)$. The visual cone of σ relative to O is the hemisphere bounded by $\mathscr{V}_O(\sigma)$ and on the same side of σ_O as σ. Note that all planes parallel to σ will have the same vanishing set, as their translation to O is the same.*

Example 2. In Figure 3 we see two planes σ, τ. The two planes are parallel to each other, hence their translations to the origin are equal and define the same geodesic when intersected with the sphere. This geodesic is their vanishing set. The visual cone of σ is the hemisphere on the side of σ relative to σ_O, and the cone of τ is the opposite hemisphere. The spherical anamorphs of each plane are obtained by joining the vanishing set to them both, so they intersect at the geodesic. Note that any plane parallel to σ has to have exactly one of these two visual cones and anamorphs, according to each side of σ_O it happens to lie.

We see that the images of both lines and planes are determined by the geodesics of the sphere. Indeed, geodesics and their rendering are the main concern of spherical anamorphosis and perspective. We therefore recall some generalities now:

Because two different planes with a common point intersect along a line, the planes of two geodesics will intersect along a diameter of the sphere, which will project as a pair of antipodal points (so the vanishing sets of two non-parallel spatial planes will always have two points in common). Conversely, two antipodal points P and $P^\star$ on the sphere define a family of planes around the axis $PP^\star$, which define a family of geodesics that covers the sphere without intersecting outside of those two points (a foliation of $S^2_O \setminus \{P, P^\star\}$). By contrast, two non-antipodal points define a single geodesic. Note that although two points of a spatial line, P and Q, define the line, giving their projections P' and Q' on the sphere only defines their geodesic, but does not determine which meridian of that geodesic is the line's anamorphic image. But giving the projection of one point of the line, P', and the projection of another point V' which is known to be a vanishing point, does determine the line's anamorph to be the meridian $V'P'V'^\star$.

Example 3. The is a classical problem in the study of both perspective and anamorphosis.

In linear perspective the various positions of the cube relative to the projection plane result in so-called one, two, and three-point perspectives of the cube. In spherical anamorphosis, the vanishing points defined by the cube are always six. There is no privileged direction of view, the sphere being isotropic, and the position of the vanishing points depends only on the orientation of the cube relative to O. Note that by proposition 1 translating the cube does not move its vanishing points (though it changes the cube's visual cone) but rotating it does. The position on the vanishing points depends only on the orientation - not the spatial position - of the edges of the cube (Figure 4).

We take note of the degenerate cases when the lines or planes do contain O. Then a line l will project as just the two antipodal points of its translation to the origin, l_O, but these points will not be vanishing points, by definition 4. Analogously, a plane σ through O will project as the geodesic $\sigma \cap S^2_O$, but this will be its full image and contain no vanishing points.

We note that definition 4 attributes a vanishing set to the anamorphic image of arbitrarily complex closed objects, not only lines and planes.

We have now a nice way to capture all the visual information around a point onto a drawing. It comes with an elegant definition of vanishing points . All of this

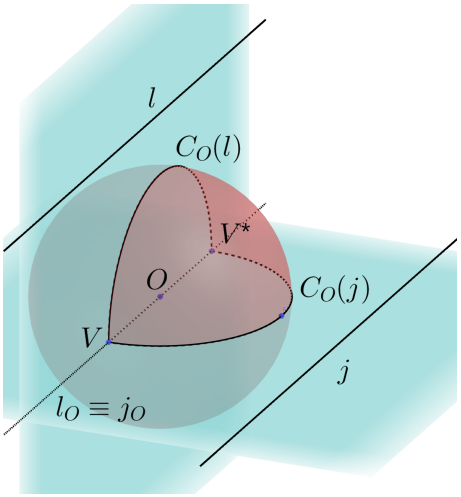

Fig. 2 Two parallel lines l, j. Their visual cones are two meridians converging at the vanishing points V and $V^\star$.

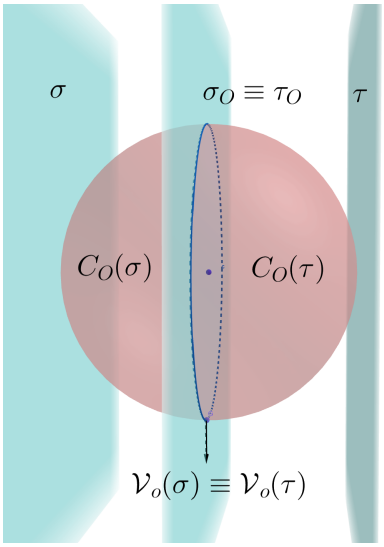

Fig. 3 Two parallel planes σ, τ. Their visual cones are two hemispheres converging at a geodesic that is their common vanishing set.

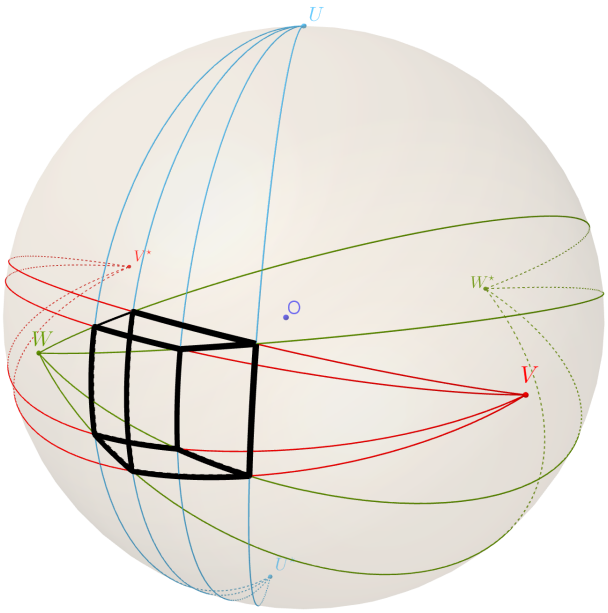

Fig. 4 The six vanishing points of the spherical anamorphosis of a cube.

followed from the principle of radial occlusion and the insistence that a drawing is a compact set. But our drawing is still on a curved surface. The passage from anamorphiosis to perspective comes simply from insisting that our drawings should be flat.

Spherical perspective as cartography of the visual sphere

We have seen how the spherical anamorphosis captures the visual information relative to a point O in the very concrete mimetic sense: it is a 2D projection that looks exactly like the original objects when seen from O.

We define a spherical perspective to be a flattening of a spherical anamorphosis, that is, a representation of it on the plane. Passing the spherical drawing to the plane will of course deform it, as is well known in cartography. So we will sacrifice the mimetic properties of the anamorphosis: the perspective drawing will no longer fool the eye. It will require interpretation. But we insist that it should preserve all the visual information, so that the anamorphosis should be in principle be recoverable from the data in the drawing - that is, one should be able to fold the perspective back onto the visual sphere. Hence, the flattening must be a bijection (almost everywhere at least). We also try to preserve at least some properties of continuity.

Here as in the previous anamorphosis step we will keep our adherence to the view of perspective as compactification. Our spherical perspectives will all be compact perspectives; they will be projections from the visual sphere to a compact subset of the plane. In this we are guided by the philosophy that compact sets are a fruitful abstraction of those things that we can actually draw, and we can only draw bounded shapes in bounded time.

We can certainly conceive of unbounded perspectives (classical perspective is one) but so can the logician conceive of infinite proofs and yet we find the concept of a finite proof to be most fruitful. Mathematics profits as much from self-imposed restrictions as from liberties. In this work our game will be this notion of a topologists view of perspective, and this restriction will prove to have its benefits. For instance, at its most prosaic, a compact representation can be stored as a raster representation in a computer file, something very useful if one is to recover the anamorphosis as a VR visualization. (Barnard 1983, p. 441) points out this advantage, calling the spherical representation ”closed” by opposition to the ”open” cartesian space, where by ”closed” he means ”bounded”. An unbounded representation would require more sophisticated ways of storing visual data, for instance through parametric forms or equations. For some graphical computing these would be inconvenient, but to the human draughtsman they are fatal. We are interested in what we can recover from the pencil marks on a single drawing. We are bound to compactness by the nature of our tools.

We now present our definition of perspective, which may seem quite abstract but will be made clear ahead through examples.

Definition 5. Let U be an open dense subset of the sphere S^2_O. We say that $\mu : U \to \mathbb{R}^2$ is a of S^2_O if μ is an homeomorphism onto $\mu(U)$, and there is a $\tilde{\mu} : cl(\mu(U)) \to S$ such that $\tilde{\mu}|_{\mu(U)} = \mu^{-1}$. We say that $p = \mu \circ \lambda_O$ is the *perspective* associated to the flattening μ, where $\lambda_O : \mathscr{R}_O \to S^2_O$ is the conical projection . Let $\tilde{p} = \lambda_O^{-1} \circ \tilde{\mu}$. Given an object Σ, we say that $\tilde{p}^{-1}(C_O(\Sigma))$ is the strict perspective image of Σ, that $\tilde{p}^{-1}(\mathscr{V}_O(\Sigma))$ is the vanishing set of Σ, and that the of Σ is the union of its strict perspective image with its vanishing set.

The following set is often useful in discussing perspectives.

Definition 6. Given a flattening μ of S^2_O, we call of μ to the subset of points of $cl(\mu(S^2_O))$ where $\tilde{\mu}$ is not injective.

The intuitive translation is that a flattening is an arbitrary map the sends the sphere (and hence the anamorphic representation of a scene) to a compact set of the plane, in such a way that it is a bijection and continuous both ways "". The exception is the blowup set, where the flattening is not defined. But the blowup set is of measure zero, that is, it is at most one-dimensional, hence the anamorphic picture can be recovered by continuity.

The perspective is simply defined as the sequence of the two steps from space to plane: anamorphosis onto the sphere followed by flattening. Since the anamorphosis is always the same, each spherical perspective is completely characterized by its flattening map.

Note 3. The definition above assumes that we are projecting the whole sphere. We can easily define a to be a flattening of a compact, connected region of the sphere. Then we can include, trivially, the (hemi)spherical perspective of Barre and Flocon. In this work we found it proper to focus on the *total* spherical perspectives, that is, spherical perspectives that project the whole sphere. But partial spherical perspectives are also important in practice, since they include things like cylindrical perspective, or linear perspective onto a compact region of the plane.

Note 4. A note for geometers: the term *blowup* is not being used here with its usual significance in geometry. The name arose from the fact that in the azimuthal equidistant case (treated ahead) this set is the inverse image of a point by $\tilde{\mu}$, and equals a circle which corresponds to the tangent plane at that point in the sphere. This is analogous to the blowup of point (although not projectivised), and that is where the name comes from.

Referentials

Ahead we will study three flattenings, each of which defines a spherical perspective. In all cases some conventions will be useful, so we will set them here.

Given a point P in space, we may be concerned with its projection on the sphere, P', and then with its perspective image on the plane, P''. This notation gets rather

cumbersome, so we will instead use the following simplification: we denote both the spatial point and its anamorph on the sphere by **P**, in bold font, leaving context to disambiguate between the two, and we denote the perspective image on the plane by *P*. We will use more careful notation when ambiguity warrants, but for the most part we can identify spatial points with their spherical anamorphs.

We will need a . This is of course arbitrary, but we will choose the following in this text:

We consider a referential (x,y,z) centered at the observer's viewpoint, which we take to be $\mathbf{O} = (0,0,0)$ (see Figure 5). We take three arbitrary points on the unit sphere $S^2_{\mathbf{O}}$, denoted **R** (short for Right), **F** (Front), and **U** (Up), such that the vectors $(\overrightarrow{\mathbf{OR}}, \overrightarrow{\mathbf{OF}}, \overrightarrow{\mathbf{OU}}) = (\overrightarrow{u_x}, \overrightarrow{u_y}, \overrightarrow{u_z})$ form a right-handed orthonormal referential. We denote the antipodes of these points by **L** (Left), **B** (Back), and **D** (Down), respectively.

We call to the plane **ROF**, we call to the geodesic it defines by intersection with the sphere, and *horizontal* to any plane parallel to it; we call or to the plane **ROU** and to its geodesic we call the (or "crown", from). We call to any plane parallel to it. We call to the plane **UOF**, to its geodesic, and to any plane parallel to it. We call anterior space to everything on the same side of the observer's frontal plane as point **F** and posterior space to everything on the opposite side.

Finally, regarding spatial lines, we say a line is a if it lies in a frontal plane, otherwise we call it a . A receding line must intersect the coronal plane; if it intersects it orthogonally then we say it is a .

Note 5. Note that these notations vary widely in the literature, some author's preferring the for the reference points, using "north" in place of "front", "east" in place of "right", etc.. In the present text we opted for anatomical notation rather than geographical, as overtime we found the associated imagery clearer, especially for beginners. We mostly follow (Araújo 2018c) except where it calls equatorial plane to what we here call the coronal plane, as we feel it was mixing metaphors, and confusing, to let "equator" remain a sole geographical term in the midst of an otherwise uniform anatomical notation.

Given a spatial point **P** we will call **P**-geodesic to any geodesic that contains point **P**. But note that we will only call **P**-meridian to a meridian that goes from **P** to its antipode $\mathbf{P}^\star$.

Two spherical coordinate systems will be needed ahead, and must sometimes be related to each other. The following two sections define them. This may be skimmed now, and read carefully when the developments requires them.

Azimuthal coordinate system

This coordinate system is especially useful for the azimuthal equidistant perspective. It corresponds to the so-called except that we put our reference point **F**(ront) where the usually is in the star maps, simply because it is more convenient for the most

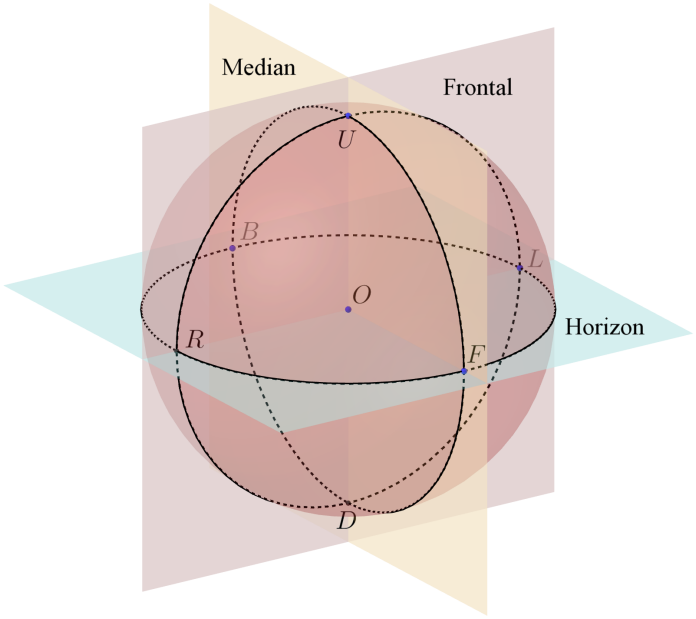

Fig. 5 Reference points and planes.

common setups of spherical perspective drawings. We locate a point **P** on the sphere by two angles θ and ζ (see Figure 6). Theta is called the and determines in which of the **F**-geodesics the point is, while zeta, often called the or , measures how far **P** is from **F** along its **F**-meridian. More specifically, $\theta = \angle \mathbf{P_F OR}$, where $\mathbf{P_F}$ is the orthogonal projection of **P** onto the observer's frontal plane, and $\zeta = \angle \mathbf{POF} \in [0, \pi[$.

In coordinates,

$$\theta = \text{atan2}(z,x), \ \zeta = \arccos(y) \tag{1}$$

where $\text{atan2} : \mathbb{R}^2 \setminus \{(0,0)\} \to]-\pi, \pi]$ is the two-argument arctangent, such that $\text{atan2}(y,x)$ is the angle between the ray from $(0,0)$ to (x,y) and the positive x-axis. Note that $\text{atan2}(y,x) = \arctan(y/x)$ when $x > 0$ and otherwise differs by the appropriate addition/subtraction of π, or by extension through continuity, in order to extend the arctangent function to the four quadrants.

Of course the azimuthal system on the sphere may be extended to a full set of spherical coordinates for $\mathbb{R}^3$ by adding the radial coordinate $\rho = \sqrt{x^2+y^2+z^2} = |\mathbf{OP}|$. In that case we have $\zeta = \angle \mathbf{POF} = \arccos(y/|\mathbf{OP}|)$ for a general spatial point **P**, which reduces to the previous expression when $|\mathbf{OP}| = 1$.

Horizontal coordinate system

The horizontal coordinate system locates a point **P** on the sphere by two angles λ and φ (see Figure 6) such that if $\mathbf{P_H}$ is the orthogonal projection of **P** onto the plane of the horizon, then $\lambda = \angle \mathbf{P_H OF}$ and $\varphi = \angle \mathbf{POP_H}$. We will call lambda the and phi the . Intuitively, to locate **P**, we start at **F**, rotate our gaze around the z axis by the angle λ until facing the vertical plane through **P**, and lift our gaze by an angle φ to face **P**. This is of course the system that surveyors ordinarily use, and is naturally adapted for measuring from nature using theodolites, clinometers, and other surveying equipment (see for instance Schofield and Breach (2007)).

In coordinates we have

$$\lambda = \operatorname{atan2}(y,x), \ \varphi = \arcsin(z) \tag{2}$$

and adding the radial coordinate ρ we obtain a general spherical coordinate system for $\mathbb{R}^3 \setminus \mathbf{O}$, with $\varphi = \arcsin(z/|\mathbf{OP}|) = \arcsin\left(z \Big/ \sqrt{x^2+y^2+z^2}\right)$.

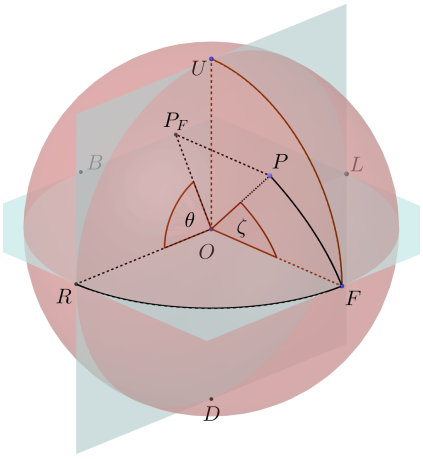

Fig. 6 Azimuthal coordinate system. A point P on the sphere is determined by angles θ (azimuth) and ζ (zenith angle, or polar angle).

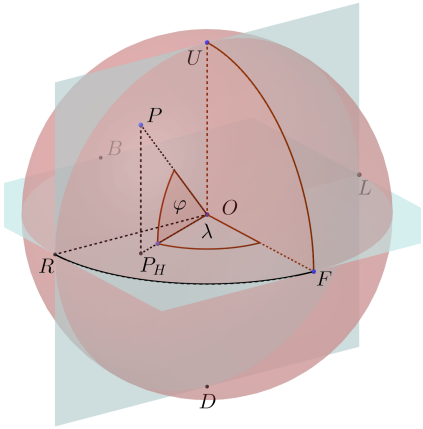

Fig. 7 Horizontal coordinate system. A point P is determined by angles λ (bearing) and φ (elevation).

We note that in drawing practice it is useful to measure angles (and distances along **F**-meridians) in degrees rather than radians, and we will follow this practice.

Angular measurements

In order to draw spherical perspectives one must take , such as an astronomer or surveyor would, and then render their projections according to the rules of the perspective. When drawing from nature these angular measurements can be taken with adequate devices - such as theodolites, physical or digital - or, with greater error, by very simple methods such as using a pencil or even one's hand as reference. An old astronomer's trick is to stretch the arm straight ahead, rotate the palm away from the eye with the knife of the hand facing upwards. In this position, the hand should subtend about ten degrees of the field of view when measured vertically along the line of the knuckles. Of course this rule-of-thumb must be calibrated to one's own body proportions, but it is good enough for casually take measurements for an outdoor sketch.

The measurement as described obtains the angular elevation. Rotating the hand until the knuckles are horizontal allows you to similarly measure the bearing. So this is appropriate for the horizontal coordinate system. Measuring angles in this system is somewhat natural, and the horizontal system is the one commonly used in surveying (Schofield and Breach 2007), for which there is no shortage of tools, both mechanical and digital.

Measuring angles directly in the azimuthal system is rather more awkward, but up ahead we will see how horizontal system measurements may be easily converted to azimuthal measurements at key points of the drawing. So in either case the horizontal system is the one most often used to obtain the raw measurements of a drawing.

Azimuthal equidistant spherical perspective (360-degree Fisheye)

We will first consider the case of the . As we have seen in definition 5, a spherical perspective is defined by its flattening (and often, as in the present case, named after it). So we must begin by defining the flattening.

The azimuthal equidistant flattening

We consider the flattening defined by the azimuthal equidistant map. This is the projection used by Barre and Flocon for their fisheye perspective (Barre and Flocon 1968). The flattening far antedates the perspective, having a long history in the cartography of both Earth and night sky. call it the , as is usual in France, where it is named in honour of Guillaume Postel, who used it in a 1581 map, but it had in fact been used much earlier by several authors. The earliest extant example is a star map of 1426 by Conrad of Dyffenbach, and several others use it before Postel, including Albrecht Durer in a 1515 map and Mercator as an inset for north polar areas on

his 1569 navigational map (Snyder 1993, p. 29). According to Berggren (1981) it had already been described in principle, with an emphasis on its uses for celestial mapping, by al-Biruni in the 10th-century, who in turn attributes its origin to other authors of the ninth century (Savage-Smith 2015, p. 35-36)). Snyder mentions that it *may* have been known to the ancient Egyptians and used for star maps. It is in fact eminently suited to that function, since it preserves angular distances from the zenith. Although this flattening of the sphere is well known in cartography, it has been derived again and again by multiple authors interested in spherical perspective (the present one included) either out of ignorance of its existence or the need to express it in some particular convenient form. We here express it in a way especially useful for our purposes.

The can be defined by the following requirements:

1. Maps **F** to $(0,0)$.
2. Maps **F**-geodesics to line segments.
3. Preserves lengths along **F**-geodesics.
4. Preserves tangents at **F**.

Let's consider intuitively how to make such a flattening. The sphere may be seen as the union of all the **F**-meridians, that is, all the meridians going from **F** to its antipodal point **B**. Now imagine that the meridians are inextensible threads, and suppose that, keeping them fixed at **F**, you release them from **B**, and straighten them without stretching on the sphere's tangent plane at **F**, all the while keeping each meridian on its original plane through **OF**. Then you will have transformed the sphere of unit radius into a disc of radius π, satisfying the conditions above (see Figures 8 and 9). Then **F**-meridians will be distributed radially, and distances along them will equal angular measurements from **F**. of the **FB** axis, that is, circles of the sphere which are parallel to the frontal plane, will project as uniformly spaced circles. In particular, the **URD** is a circle with half the diameter of the projection disc. The (the space in front of the observer) will project onto the bounded by the corona *URD* and the (the space behind the observer) will project onto the ring between the corona's circle and the outer rim of the .

Analytically, the flattening may be seen as a two step process: Given a point $\mathbf{P} = (x,y,z)$ on the sphere we project it onto the observer's frontal plane to get $\mathbf{P_F} = (x,z)$. This determines the plane of the **F**-meridian containing **P**. We then scale this projection to a length of $\arccos(y)$, to preserve the angular measure of **P**'s position along the **F**-meridian. This defines a map $\mu : S^2_O \setminus \{\mathbf{B}\} \mapsto \mathbb{R}^2$ by $\mu(\mathbf{P}) = \mathbf{P_F} \arccos(\overrightarrow{\mathbf{OP}} \cdot \overrightarrow{\mathbf{OF}})$, or, in coordinates,

$$\mu(x,y,z) = \frac{(x,z)}{\sqrt{x^2+z^2}} arccos\,(y) \tag{3}$$

which is a flattening according to definition 5. Indeed, it is a homeomorphism from the dense subset of the sphere $U = S^2_O \setminus \{\mathbf{B}\}$ (the sphere minus the "**B**ack" point) to the open disc $\mathscr{D} = \{(x,z) : \sqrt{x^2+z^2} < \pi\}$. According to definition 6 the blowup set is the outer perimeter of the disc, $\mathscr{B} = cl(\mathscr{D}) \setminus \mathscr{D} = \{(x,z) : \sqrt{x^2+z^2} = \pi\}$, and

the inverse of μ can be extended by continuity to a map $\tilde{\mu} : cl(\mathscr{D}) \mapsto S^2_O$, by setting $\tilde{\mu}(P) = \mathbf{B}$ for all $P \in \mathscr{B}$.

The , which gets entirely mapped by, $\tilde{\mu}$ to point **B**, can be seen as the replacement of the point **B** by a circle that represents the tangent plane of the sphere at **B**. Each point of the circle is connected by an F-meridian, representing a direction from which B may be approached. So, every radius from F to the rim of the disc is a line from F to B, but each such line codifies a different direction from which B may be reached along the sphere. The term *blowup* is borrowed from the analogous procedure in the study of singularities, wherein a point is replaced by a projective line.

This flattening is very natural when expressed in the azimuthal coordinate system we described above. It maps (θ, ζ) to $\zeta(\cos(\theta), \sin(\theta))$, that is, (θ, ζ) act as polar coordinates from the sphere to the perspective picture plane.

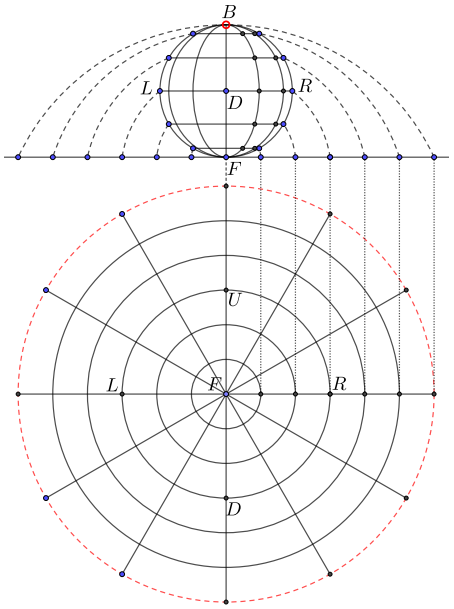

Fig. 8 The azimuthal equidistant flattening. Side and top views. Distances are preserved along **F**-meridians and angles are preserved at F.

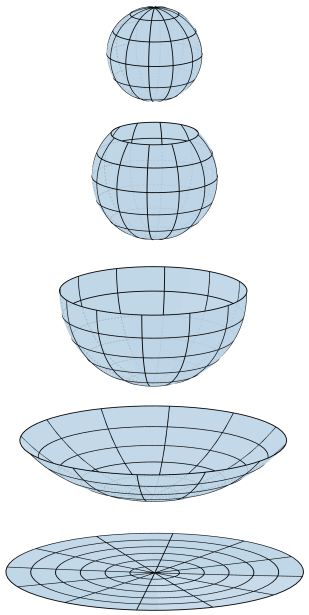

Fig. 9 Several steps in flattening the sphere onto a disc. The sphere is pierced at B and the meridians straightened onto the tangent plane at F.

Solving the azimuthal equidistant spherical perspective

Now that we have defined the azimuthal equidistant flattening, the corresponding perspective is intrinsically defined: to obtain the perspective image of a spatial point P, first project it radially to the sphere by doing $P \mapsto \overrightarrow{OP}/|\overrightarrow{OP}|$ and then flatten it to the plane. Given a scene, a computer could render it easily pixel by pixel, using equation 3. Since occlusion is radial in spherical perspective, even the usual would still work for rendering 3D scenes. But is a more complicated process that must be handled with judgment. How can you *efficiently* perform the necessary measurements and renderings if you can only handle dozens rather than millions of operations?

In the following we will be concerned with solving this perspective. By the term "" we mean to obtain a systematic procedure for drawing all line images, plane images, and their vanishing sets, for an arbitrary scene, using simple geometrical operations that a human draughtsman may reasonably perform.

Following Araújo (2018c), we will follow the strategy of classifying geodesics and using this as a basis for rendering all other objects. It is important to realize that the classification is not unique; it is a matter of convenience. Different partitions of the set of geodesics may be adapted to different strategies for rendering the perspective images of lines, planes, and their vanishing points.

Theorem 3 gives us a simple in this perspective, with two classes.

Lemma 1. *Two geodesics intersect at exactly two antipodal points.*

Proof. Let g_1, g_2 be geodesics defined by the planes H_1, H_2. Since both plane contain O then they intersect on a line through O, which must therefore intersect the sphere at two antipodal points belonging to both geodesics.

Proposition 3. *In azimuthal equidistant perspective, a geodesic is projected as either a diameter of the perspective disc or an F-starred, closed curve.*

Proof. Recall that, given a point P, a set is called P-starred if any ray from P intersects the set in one point at most. Let g be a geodesic not passing through $\mathbf{F}$ and H its plane. Since g doesn't contain $\mathbf{F}$ then it doesn't contain $\mathbf{F} = \mathbf{F}^\star$. The $\mathbf{F}$-geodesics are a foliation of $S^2_O \setminus \{\mathbf{F}, \mathbf{B}\}$. By lemma 1, g intersects each F-geodesics at exactly two antipodal points, none of which is $\mathbf{F}$ or $\mathbf{B}$. Hence it intersect each FB-meridian at exactly one point none of which is $\mathbf{F}$ or $\mathbf{B}$. Hence its image intersects each ray of the perspective disc at a single point, hence it is F-starred, and it is continuous and closed because the geodesic is continuous and closed and the flattening is continuous in $S^2_O \setminus \{\mathbf{B}\}$. As for geodesics through $\mathbf{F}$, they must project as diameters by the definition of the azimuthal equidistant map.

Let us investigate the aspect of these curves by ((Hohenwarter et al 2013) code and available at the author's website Araújo (2015)). In Figures 10 and 11 we can see the family of $\mathbf{LR}$-geodesics and its perspective image. The family has been plotted at 5-degree intervals of polar angle ζ at the median line, from the horizon at polar

angle $\zeta = 0°$ to the corona at $\zeta = 90°$. Each **LR** geodesic projects on the perspective as a continuous, closed, convex, F-starred curve. The corona projects as a circle with half the radius of the perspective disc, and then as ζ decreases and the anterior part of the projected curve becomes flatter but still fairly circular in nature, the posterior part (on the ring outside the corona) of the curve bulges to hug the line LR closer and closer as the geodesic approaches the horizon. The tangent at L and R becomes closer and closer to the horizontal until finally at $\zeta = 0°$ the geodesic reaches the horizon, which no longer projects as an F-starred curve, but instead collapses into a diameter of the disc.

Each geodesic divides the into a region and a non-convex complement. Note that both these regions are the images of planes, or rather of equivalence classes of planes parallel to each other (since they all have the same vanishing set which is the geodesic itself). The planes that are inside the convex region are antipodal to the ones represented by the outer region - they are parallel but face opposite sides of the sphere.

These geodesic images are rather complex curves in appearance and ahead we will consider how to plot them by elementary means in close approximation. For now we will take them as given and consider the uses of these plots.

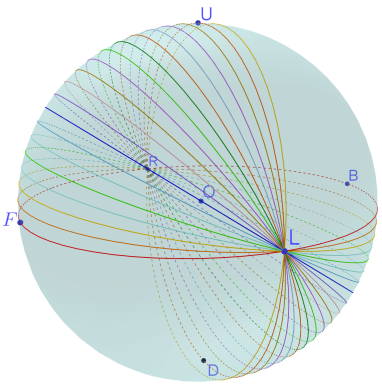

Fig. 10 The **LR** family of geodesics, plotted at 5 degree intervals of polar angle along the median line.

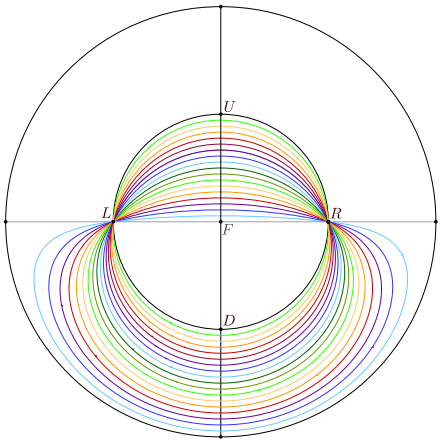

Fig. 11 The image of the **LR** family of geodesics under the azimuthal equidistant perspective.

Fixed grids for the azimuthal equidistant perspective

A simple way of drawing spherical perspectives is by . One can parametrize a finite number of horizontal and vertical lines on frontal planes, at regular intervals of elevation and bearing respectively, and plot them through equation 3 to some required

precision. Then any point may be obtained in approximation by locating it on this grid, to whatever precision it allows.

In fact the ordinary literature on spherical perspective for artists uses such almost exclusively. The most sophisticated use of is probably what can be found in (Michel 2013), and the intricate works therein make obvious that such methods can be perfectly adequate for many artistic applications. Let us therefore consider the construction of such grids.

Instead of parametrizing horizontal and vertical lines, we note that the family of **LR** geodesics we presented above is all that we need to print an adequate grid. Consider a **LR**-geodesic that crosses the anterior median line at a polar angle ζ, say the $\zeta = 45^\circ$ in Figures 10 and 11. This may be interpreted as a pair of diametrically opposite frontal lines: the anterior meridian of the geodesic is the projection of a horizontal frontal line that crosses the median line in front of the observer at a 45° elevation, that is, at point $(\theta = 90^\circ, \zeta = 45^\circ)$ and goes to the vanishing points L and R. On the other hand, the posterior meridian of the same geodesic (the antipodal image of the first meridian) can be seen as the image of a horizontal spatial line going from R to L, that crosses the median line behind and under the observer, at a negative 45° elevation, or at point $(\theta = -90^\circ, \zeta = 135^\circ)$, that is, at the antipode of the first point. The meridians of these two lines are antipodal of each other, and together form a complete geodesic. Repeating the plot of the FR-family for negative ζ at the frontal median line, we obtain a symmetrical family of horizontal line plots, and this forms a full plot of horizontals.

Now consider the F-family of geodesics, which as we have seen project as diameters. Each diameter can be interpreted as a pair of lines that go from F to B, perpendicular to the coronal plane (central lines). Each diameter will represent two antipodal line images, say one passing the coronal plane to the left and above the observer, and the other passing to the right and below the observer along the same plane through **O** and perpendicular to the coronal plane. We plot these diameters crossing the corona at regular intervals of θ.

Since, as we have seen above, each ray from F in the perspective disc intersects each LR geodesic exactly once, then the set of F rays together with the set of LR geodesic images forms a grid on the perspective disc, such that any point may be located at the intersection of two such lines.

In Figure 12 (left) we see a grid where we plotted these two classes of geodesics at 15-degree intervals. This can be interpreted either as grid of geodesics or as a grid of horizontal and frontal lines. In either case they locate any point on the sphere up to the precision determined by the grid interval.

As mentioned previously, a crucial part of treating a perspective is to consider the classes into which one should divide the set of geodesics. The partition is not unique. In the present case one might as well choose a grid of crossing LR and UD geodesics (interpreted as horizontal and vertical lines) as in Figure 12 (right). The UD geodesics are readily obtainable from the set of LR geodesics in Figure 11 by a 90° rotation around F.

We will see ahead that the set of LR geodesics is even more versatile than that: it can be seen as a seed for the set of all geodesics.

But for now this is enough of grids. Thinking in terms of grids is a limitative view of perspective, both classical and spherical. In the next section we will develop spherical perspective as a perspective proper, in the vein of Barren and Flocon's treatise (Barre and Flocon 1968) and then generalize it following Araújo (2018c). Only after that we will revisit grids, in a new way that makes them dynamic rather than fixed and exploiting the symmetries of the perspective.

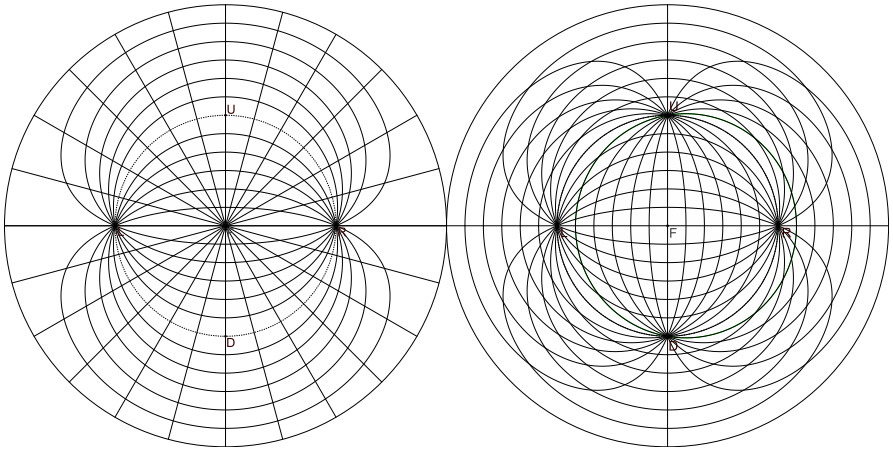

Fig. 12 Geodesic grids. Left: Grid of *LR* and *FB* geodesics. Right: Grid of *LR* and *UD* geodesics. All geodesics plotted at 15-degree intervals.

Note 6. While we focus here, for conceptual reasons, on grids of geodesics, there are other useful spherical grids made up of non-geodesic folliations: Figure 8 shows a grid of constant polar angle circles crossing *LR* geodesics, and the curves of constant elevation that together with *UD* geodesics make a very useful grid (see Araújo (2018c)).

A ruler and compass construction of the azimuthal equidistant spherical perspective

We will now lean to draw geodesics (and images of lines and planes) by ruler and compass constructions. We do this in two parts. In the first part we follow Barre et al (1964) to render the anterior hemisphere by . In the second part, we follow Araújo (2018c) in generalizing these constructions to the posterior hemisphere through the use of antipodal images.

A crucial point in the work of Barre et al (1964) is that in the anterior disc the geodesic projections are well approximated by arcs of circle, and their perspective constructions are all built under that approximation. In fact it is a matter of definition

whether the of Barre and Flocon is the azimuthal equidistant perspective or another one, defined by projection of geodesics in exact arcs of circle. Either way, they are functionally the same. The point of using arcs of circles is that they are very nice objects to work with, being the very next step in complexity from line segments: a line segment has zero curvature, while an arc of circle has constant curvature. Two points determine a line segment, while three points determine an arc of circle. Our goal in rendering lines in the anterior hemisphere consists in finding a set of three adequate points to define their arc of circle image.

We start by noticing that points in the coronal plane are very easy to render.

Proposition 4. *If* **P** *is on the coronal plane, then its perspective image P is on the coronal circle and* $\angle PFR = \angle \mathbf{POR}$.

This proposition follows trivially from the form of the azimuthal equidistant flattening, but it suggests a very important construction that relates the spherical perspective and the . This is crucial for drawing from , just as in classical perspective.

Construction 1 . *Let* $\mathbf{P} \neq \mathbf{O}$ *be a point on the coronal plane. Draw an orthographic projection of the 3D scene, onto the coronal plane, on the same drawing as the perspective disc, with F serving both as the perspective image and as the orthogonal image of* **F**. *Then, if P is the perspective image of* **P** *and* P_f *is its orthogonal projection onto the coronal plane, P is the intersection of the ray* $\overrightarrow{OP_f}$ *with the perspective image of the corona (see Figure 13). Note that the orthogonal perspective may be scaled at will relative to the perspective disc.*

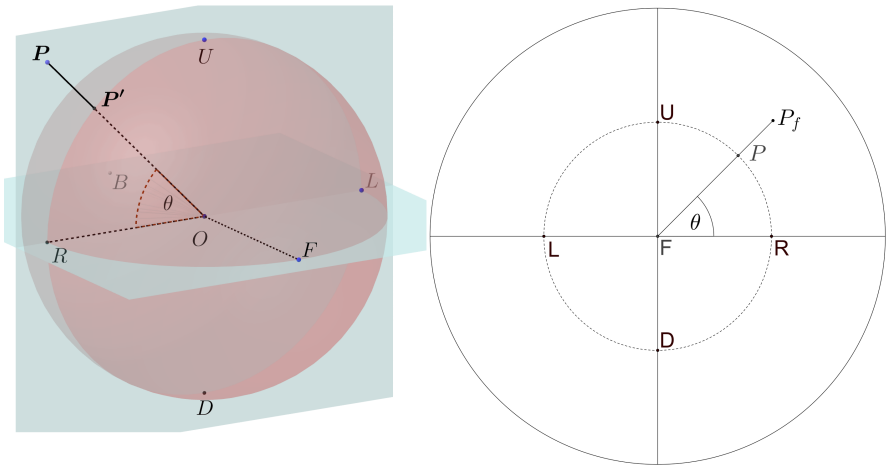

Fig. 13 The perspective image of a point **P** on the coronal plane is the point P on the image of the corona such that $\theta = \angle PFR = \angle \mathbf{POR}$. This may be obtained directly by drawing a line from F to P_f, the orthogonal projection of P on the coronal plane, arbitrarily scaled at will and overlayed on the perspective plane with F's perspective image coincident with its orthogonal image.

We are now ready to construct the images of lines in the . Following Barre and Flocon (1968) we divide them into two classes: receding (intersecting the coronal plane) and frontal (parallel to the coronal plane). In particular, receding lines may be central, that is, have F and B as vanishing points.

Construction 2 . *Suppose l is a central line. Then it intersects the coronal plane at a point* **P**. *Let P_f be the frontal orthographic projection of* **P**. *Then the anterior image of l is the radius of the anterior disc that goes through P_f.*

Proof. Since l is a central line then it has F as a vanishing point and must project as a radius. By construction 1, it must contain P_f.

Construction 3 . *Let l be a line on an anterior frontal plane. Then l has two antipodal vanishing points V and $V^\star$, obtained by translating l to O and intersecting it with the sphere. Since l is frontal, its vanishing points lie on the corona. Plot them as in construction* 1. *Also, l must intersect either the median plane or the horizon. Since both the median plane and the horizon define F-geodesics, angles are preserved along their images. Hence if* **P** *is a point of l on the horizon (resp. median plane) then P is a point on the horizontal (resp. vertical) diameter of the perspective disc such that $|FP| = \angle\mathbf{POF}$. Then line l projects on the anterior plane as a the arc of circle $VPV^\star$. If l is in the coronal plane then it projects as one half of the coronal circle.*

In particular we now can construct horizontal and vertical lines in the anterior half space. They just project as LPR (resp. UPD) where P is the point where the line intersects the median plane (resp. horizon).

Note that we like to measure the points where the lines cross the median plane or the horizon because at those positions the polar angle is the same as the bearing or the angular elevation respectively, and as we have mentioned before, it is much more natural to measure elevation and bearing in the horizontal system than polar angle and azimuth in the azimuthal equidistant system. Through the judicious use of the median, horizon, and coronal intersections we relate the azimuthal system, which is natural for this perspective, with the horizontal system of coordinates, which is convenient for measurements from nature.

This suggests a construction for points from their orthogonal projections on the median and coronal planes:

Construction 4 . *Let* **P** *be a point in the anterior half space. Pass a frontal horizontal line and a frontal vertical line through* **P**. *Project the lines as in construction 3 to get two arcs of circle. Then P is found at the intersection of the two arcs.*

Now we can plot general receding lines.

Construction 5 . *Let l be a receding line. It will intersect the coronal plane at a point* **P**. *Plot P as in construction 1. Since P is in the geodesic of the line then so is $P^\star$, which is found diametrically opposite to P on the corona. Let l_O be the parallel to l through O. It intersects the anterior hemisphere at a point V, which is a vanishing point of l. Project V as in construction 4. Then the line image on the anterior half space is the segment PV of the arc $PVP^\star$.*

Let's see some examples of the we can obtain:

Example 4. In Figure 14 we see three lines: line $l = VPV^\star$ is on a frontal plane somewhere ahead of the observer. It makes a 30-degree angle with the horizon, going down as it goes to the right, so that its vanishing points lie on the corona and $\angle VFR = 30^\circ$. The line crosses the median plane at point P, which is at 60 degrees elevation in front of the observer and therefore is marked two thirds of the way up on the segment FU.

Line l_1 is a receding line on a horizontal plane, going 45 degrees to the right, hence it has a vanishing point V_1 halfway at the midpoint of segment FR. It crosses the corona at a 45 degree angle down and to the left of the observer, as evidenced by point P_1, such that $\angle P_1FL = 45^\circ$. Since P_1 is on the line, the antipode $P_1^\star$ must be on its geodesic, which is therefore equal to the arc $P_1V_1V_1^\star$ in the anterior disc. However, the line itself only covers the segment P_1V_1 of this arc.

Line l_2 is also receding, but is a central line, hence its vanishing point in the anterior space is point F and the line projects as a straight line segment P_2F, where P_2 is the projection on the corona of its intersection with the coronal plane, which in this case happens somewhere at a 20-degree angle down and to the left of the observer.

These constructions, along with the decision to approximate line images by arcs of circle, are the essence of the (hemi)spherical perspective of Barre and Flocon (1968). We will now consider its , following Araújo (2018c). This method piggybacks on the previous one by relying on the arc of circle approximation in the anterior hemisphere and extending the line classification and geodesic rendering through the use of antipodal images. We begin with the .

Proposition 5. *Let* $\mathbf{P} \neq \mathbf{B}$ *be a point with perspective image P. The image of the antipode of* $\mathbf{P}$ *is the point* $P^\star$ *on the ray* $\overrightarrow{PO}$ *such that* $|PP^\star|$ *equals half a diameter of the perspective disc.*

Proof. Since P and F are not antipodal, they define a single F-geodesic, which projects as a diameter of the perspective disc. To find $\mathbf{P}^\star$ from $\mathbf{P}$, one must move 180 degrees along this geodesic (see Figure 15). Hence, since lengths are preserved on F-geodesics, then $|PP^\star|$ must equal half a diameter. Since the projection is continuous it must preserve the ordering of points, so $P^\star$ must be across from O on the projected geodesic, therefore on $\overrightarrow{PO}$.

Now we can draw a posterior meridian from a given anterior meridian.

Corollary 1. *Let g be a geodesic and m a meridian image in the anterior perspective disc. Then* $m^\star$*, the of m is the of the points* $P^\star$ *determined by proposition 5 for P in m, and we have* $g = m \cup m^\star$.

Construction 6 . *Let m be the arc of circle approximation of an anterior meridian m of a geodesic g. Mark points* $Y_i, i = 1 \ldots n$ *at regular angular intervals along m. Drawn the antipodes* $Y_i^\star$ *according to proposition 5 and interpolate a smooth curve between them to draw an approximation to* $m^\star$.

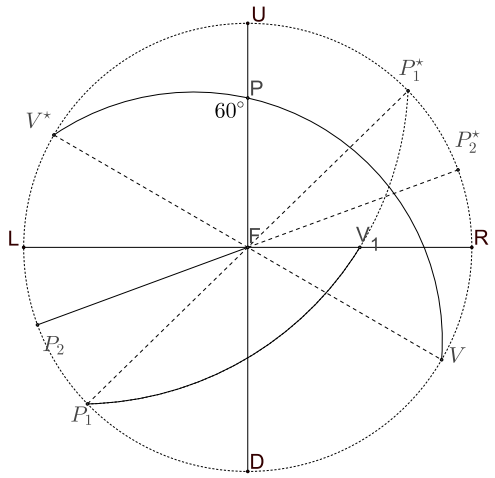

Fig. 14 Three lines rendered in the anterior half space following the method of Barre and Flocon (1968).

The interpolation in construction 6 may be done in several ways. Araújo (2018c) uses so-called , that is, sequences of overlapping arcs of circles between sequential triples of reference points $Y_i^\star$, in the sequence $Y_1^\star Y_2^\star Y_3^\star$, $Y_2^\star Y_3^\star Y_4^\star$, etc., so that each triple shares two points with the previous one. The corresponding overlap of the arcs serves as a guide for the accuracy of the approximation. If the arcs do not align well enough at the overlap (if the line is "fat") then this serves as a warning to further sub-divide the offending region of the meridian, adding further points Y_i to the list of points that generate the locus, until a required accuracy is reached. This can be done to the specific areas identified, since the required density of points will not be equal along all areas of the meridian, curvature changing faster near the corona than elsewhere.

For the draughtsman, the hardest part of the process is the theoretically more prosaic: drawing the arcs between the triples takes time and effort using ruler and compass by the usual euclidean method of taking perpendiculars through the segment midpoints to find the arc's center. But any trained draughtsman may in practice abbreviate that part by just eyeballing constant curvature arcs through each set of three given points.

Of course, other interpolation methods may be used to join the points. For instance arcs may be drawn without overlap, using the matching of end tangents to judge accuracy; Bezier curves, which are easily drawn by hand, may be interpolated instead of arcs of circles, and, of course, many draughtsmen will in practice just reach for their french curves, curve guides, or flexible curves, and judge the approximation by eye.

Apart from fatlines, Araújo (2018c) proposes a mechanical method for very quick drawing with excellent accuracy, called "".

Construction 7 *Stick a nail through the drawing at point F. Suppose a meridian m is given in the anterior disc. Suppose the perspective disc has radius r in the drawing sheet. Take a ruler marked at length* 0 *and at lenght r. Move the* 0 *mark of the ruler over the arc of the meridian m, while sliding the edge of the ruler against the nail, so that it never stops touching it; then, by proposition 6, the r mark of the ruler will describe the locus of $m^\star$. This provides a very quick and accurate way of plotting as many points as required of the antipodal meridian. Just slide the ruler as described, stopping along the way to mark as many points as desired and then interpolate by hand.*

It is quite easy and efficient to perform the process as described, as you only need to keep the eye on mark 0 and feel the contact of the ruler against the nail to make sure the ruler is properly positioned to draw the locus of $m^\star$ at the other end. One could further conceive of a simple mechanism to drawn the locus automatically and continuously as the 0 mark follows the meridian m: a ruler with a lengthwise slit wherein the nail could slide, with pencils at both marks. But the method as described is efficient enough and requires only ordinary drawing tools (apart from the nail).

We now generalize the constructions of lines to the full perspective disc:

Construction 8 . *Suppose l is a central line. Then it intersects the coronal plane at a point P. Plot this point according to construction 1. The image of l is the radius of the perspective disc that goes though P.*

Construction 9 . *Let l be a line on a frontal posterior plane. Then l has two antipodal vanishing points V and $V^\star$ on the coronal geodesic. Plot them as in construction* 1. *Also, l must intersect either the median plane or the horizon at some point behind the observer. If $\mathbf{P} \in l$ is on the horizon (resp. median plane) then P is a point on the horizontal (resp. vertical) diameter of the perspective disc such that $|FP| = \angle\mathbf{POF}$. Obtain $P^\star$ by the construction in proposition 5. The arc $m = VP^\star V^\star$ is the image of the anterior meridian of the geodesic through l. Draw m by construction 3. Draw $m^\star$ by construction 6 to obtain the image of l.*

Construction 10 . *Let $\mathbf{P}$ be a point in the posterior space, let v and h be the frontal vertical and frontal horizontal through $\mathbf{P}$, and P_H, P_M the perspective images of their respective orthographic projections in the horizon and in the median plane. Plot $P_H^\star$ and $P_M^\star$ by proposition 5. Pass a frontal vertical v' through $P_H^\star$ and a frontal horizontal h' through $P_M^\star$ as in construction 4. These intersect at $P^\star$. Construct the full geodesics of v' and h' by construction 6. These geodesics will contain v and h, and intersect at P. Alternatively, if the full geodesics are not required, just obtain $P^\star$ by proposition 5 once P is obtained.*

Construction 11 . *If l is a receding line then it has a point image P at the coronal line and a vanishing point in each of the hemispheres. If the posterior vanishing point V is given, construct the anterior vanishing point $V^\star$, according to the way V is*

given. If the plot of V is known, use proposition 5, if the orthographic projections of an anamorph point of V are known, use construction 10. Draw the anterior meridian $PV^\star P^\star$ by construction 5. Then draw the full geodesic of l through construction 6. The image of l is the subset $VPV^\star$ of the full geodesic.

Example 5. Figure 16 illustrates the use of the preceding constructions in obtaining the antipodal of line l and the prolongations to the posterior hemisphere of lines l_1 and l_2 from example 4.

It is often useful, especially in the plotting of vanishing points, to use the horizontal coordinate system. To use it graphically it is necessary to know how to plot the lines of constant elevation (the lines of constant bearing are just vertical planes through O so we already know how to plot them). The following proposition solves this in the anterior hemisphere, following Barre and Flocon (1968):

Proposition 6. *Let* **h** *be a circle of constant elevation φ on the visual sphere around O. Then h intersects the median line at the point P_M such that $|P_MF| = \varphi$, and intersects the corona at points P_L and P_R such that $P_LFL = P_RFR = \varphi$. The anterior image of h is approximated by the arc of circle $P_LP_MP_R$.*

In the posterior hemisphere we use the following proposition, following Araújo (2018c):

Proposition 7. *Let* **h** *be a circle of constant elevation φ on the visual sphere around O. Let $P \neq F$ be a point of h in the anterior disc. Let M be the intersection of $\overrightarrow{FP}$ with the corona. Let Q be the point such that M is the midpoint of $\overline{PQ}$. Then Q is in h. The posterior part of h is the locus of the Q thus defined by P, for all P in the anterior part of h.*

Proof. This follows from the fact that $\overrightarrow{FP}$ defines an F-meridian, hence preserves lenghts, and an F-meridian will intersect a line of constant elevation at exactly two points. These points are equidistant from the corona, since both the circle of h and the plane of the F-meridian are mirror symmetric relative to the coronal plane.

Construction 12 *To construct an approximation of a constant elevation line use the arc of circle approximation in the anterior hemisphere and then construct from it the locus of proposition 7 to use as an approximation for the posterior line.*

Note that although the result of proposition 7 is correct, the use of the arc of circle approximation in 12 leads to errors also in the posterior curve. These are mostly visible as a break of continuity of the tangent near the intersection with the coronal circle. See Araújo (2018c) for details.

Perspective constructions

The constructions we obtained above allow us to draw general scenes in azimuthal equidistant spherical perspective. Let us explore some examples of perspective constructions.

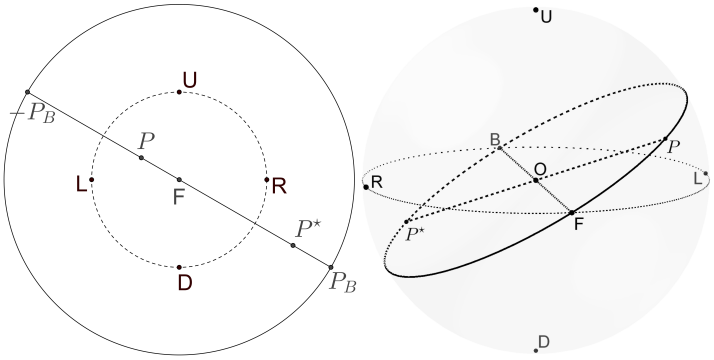

Fig. 15 Construction of antipodes. Since $\angle\mathbf{POF} = 180^\circ$ along the **FP** geodesic, then $|FP|$ equals half a diameter along the ray from P to F.

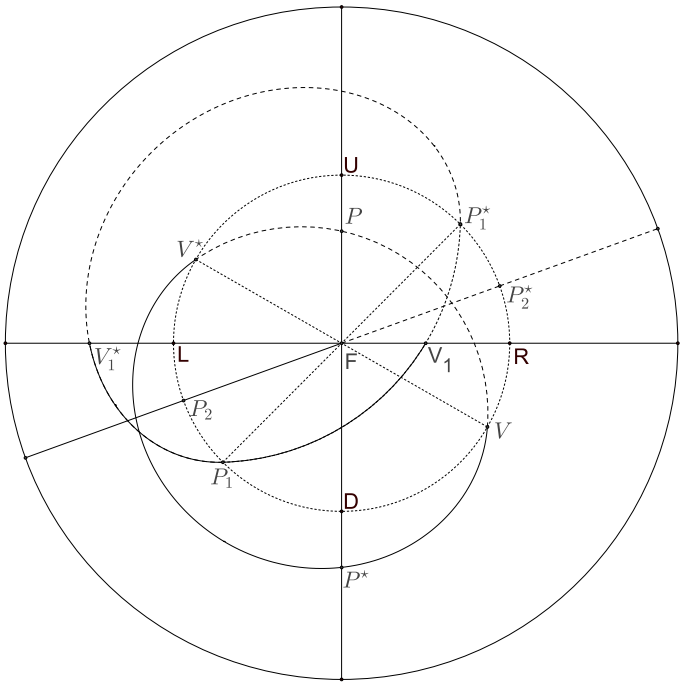

Fig. 16 Construction of lines and their geodesics on the full perspective disc according to the method of Araújo (2018c).

Tiled floor (central)

In Figure 17 we see the (or a uniform grid), a classical problem in perspective. We assume a grid of square tiles on a plane perpendicular to the coronal plane. Assume one of the vertices of the grid is at **D** and a line q of the grid , q, is parallel to **LR**. Then the vertices of the grid on line q will intersect the coronal plane at equally spaced points $Q_i, i \in \mathbb{Z}$. The lines of the grid perpendicular to q are central lines, going back to front, hence they project as rays $\overrightarrow{FQ_i}$. To find the lines of the grid going left to right, we use exactly the same trick as in classical perspective: we pass a horizontal line through D, going at 45 degrees to the grid lines. Then it will intersect exactly one vertex of the grid per row. To mark this line, place its vanishing point V at the midpoint of FR. Since the line passes at D, its geodesic also passes at $U = D^\star$. Draw the full geodesic g as in construction 6. The vertices of the grid will be at the points $G_i, i \in \mathbb{Z}$, where g intersects the central lines of the grid.

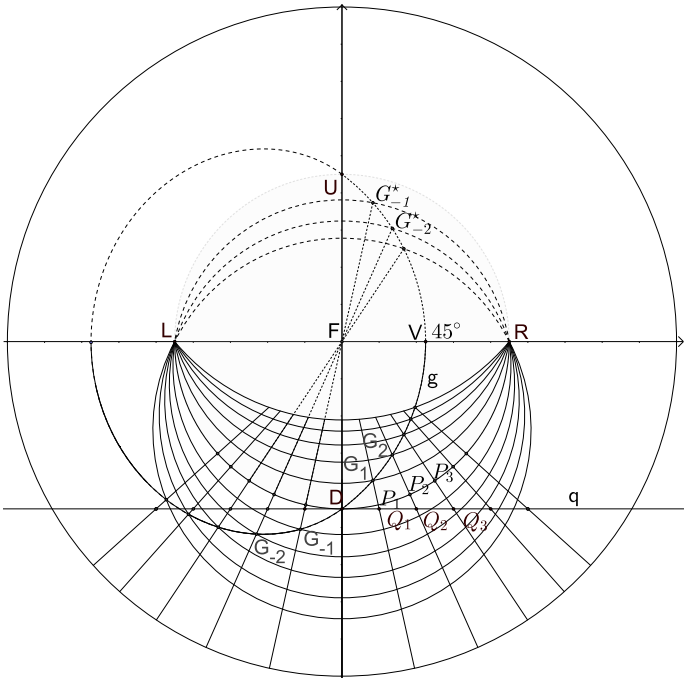

Fig. 17 Construction of a uniform central grid.

Inside a cube

In Figure 18 we show the seen from its center. The whole construction is done through the use of a 45-degree geodesic as the one in the previous example, which crosses the vertices of the room. Note that we have shaded the planes of the walls with the exception of the back wall which ends at the blowup - the resulting region is shaped like a four leafed clover. Notice the extreme distortion in the back wall, which nonetheless doesn't preclude an accurate construction by the techniques here presented.

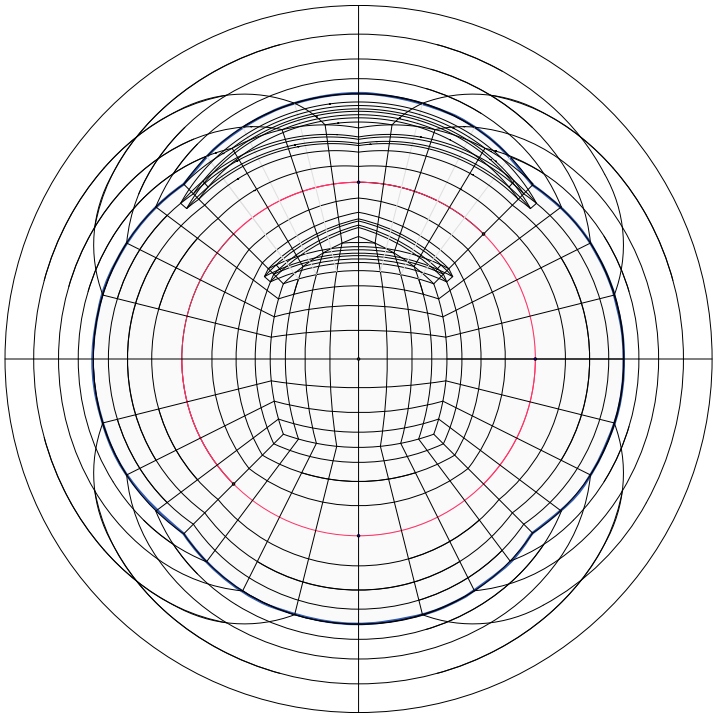

Fig. 18 Construction of a cubical room from 45-degree geodesics.

Arbitrary square

In Figure 19 we show the on the horizontal plane through **D**, in this case slanted at a 30 degree angle to the **OF** axis. We draw the orthographic top view of the square at the bottom of the Figure, at a convenient distance from the perspective drawing. Line h is a top view of the coronal plane. We extend the four sides of the square along their lines, find the intersections of these with h, and then lift these

intersections to their orthographic image of line h on the perspective disc itself, using construction 4 to get their images at the coronal circle. These four lines are all examples of receding lines, so we use their intersections with the coronal plane, and their antipodes, together with their vanishing points at 30° to the right and 60° to the left on the horizon, to obtain the images of all four lines. Their intersections determine the image of the square $ABCE$.

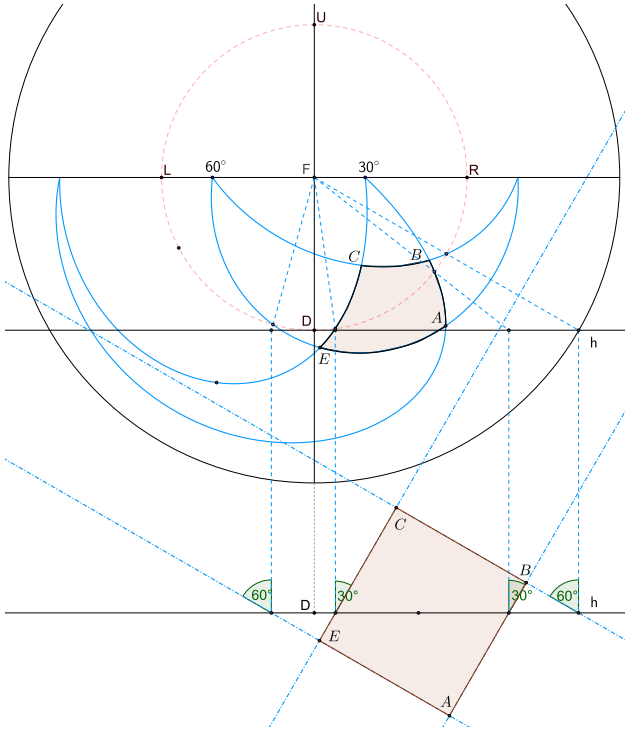

Fig. 19 A square on the ground. Spherical perspective view (Top) constructed from the orthographic projection onto a horizontal plane (Bottom).

Tiled floor

In Figure 20 we show how to multiply the arbitrary square we designed in Figure 19 to get a that is not aligned with the central axis. In this case we get a grid on a horizontal plane, whose axes go to a vanishing point V 30 degrees to the right of F and the other axis to vanishing point W at 60 degrees to the left. Starting from square $ABCE$, we pass two lines a and b at 45 degrees to the edges of the square, going to vanishing point Z at 75 degrees to the right of F and to its antipode at 105 degrees to the left of F. In the orthographic view we see how these lines are used to

obtain the grid: edge AB is extended until it hits line a. At the point P_1 where it hits a is a vertex of the grid, and two crossing lines of grid are obtained by passing a line from P_1 to the vanishing points V and W. One of these lines will hit line b, obtaining another point P_2, and the process repeats. The same thing happens in the opposite direction, obtaining the points P_{-1}, P_{-2}, and so on. In each case, one obtains a line that ping-pongs between lines a and b, and at each collision locates another vertex of the grid, which in turn generates two lines of the grid. In this way the whole grid is obtained by (Figure 21).

A fundamental departure from the classical method adopted in Figure 17 is that we don't use the orthographic projection to plot the points P_i, which is convenient as these points quickly extend beyond the boundaries of the drawing sheet, as they similarly did in the grid of Figure 17 or indeed in classical perspective. By contrast, in Figure 20 all the constructions beyond the first square and the lines a, b are , that is, are done directly from the points in the perspective disc without requiring external auxiliary diagrams. This makes the construction method compact, like the end result itself and is therefore more in accord with the general philosophy of spherical perspective.

In Figure 22 we added cubes and a ramp to Figure 21 in an example of the use of vanishing planes and constant elevation lines. Consider first the , drawn on the right side of the picture. Its base occupies 2×5 square tiles. The long axis of the base goes towards the horizon, to vanishing point V at 30° to the right of F. Suppose the ramp has a slope of 45°. Consider the proximal vertical plane that contains the long side of the ramp. Since the plane is vertical and contains the base line going to V, its vanishing plane is the geodesic through VU. Since the sloping edges l of the ramp rise at 45° from the ground, their translation to the origin, l_O, rises at 45° from O with respect to the horizon. Hence it is on the 45°. We draw that line of constant elevation by the construction of proposition 6 and denote it by c in Figure 22. The vanishing point V' of the sloping edges is in the intersection of UV with c. We draw the ramp by sending lines from the base to V' and stopping them when they hit the vertical coming from the base of the ramp.

Now consider the three box-like figures center and left of the picture. All three represent cubes of exactly the same size, which is a testament to how much the deformations of this perspective may be disconcerting with regard to one's intuitive judgment of size relations.

In all three cases a base was established that is equal to 3×3 squares. The left-most cube stands on this base, while the others are aligned with theirs by vertical lines. To establish the height of the cubes one just has to note that on each face of a cube, opposite vertices are connected by a diagonal making a 45 degree angle with the edges of the cube. Therefore, to establish height, send such a diagonal from a base vertex to its vanishing point, and the top vertex will be at the point where the diagonal hits the distal vertical of the same face of the cube.

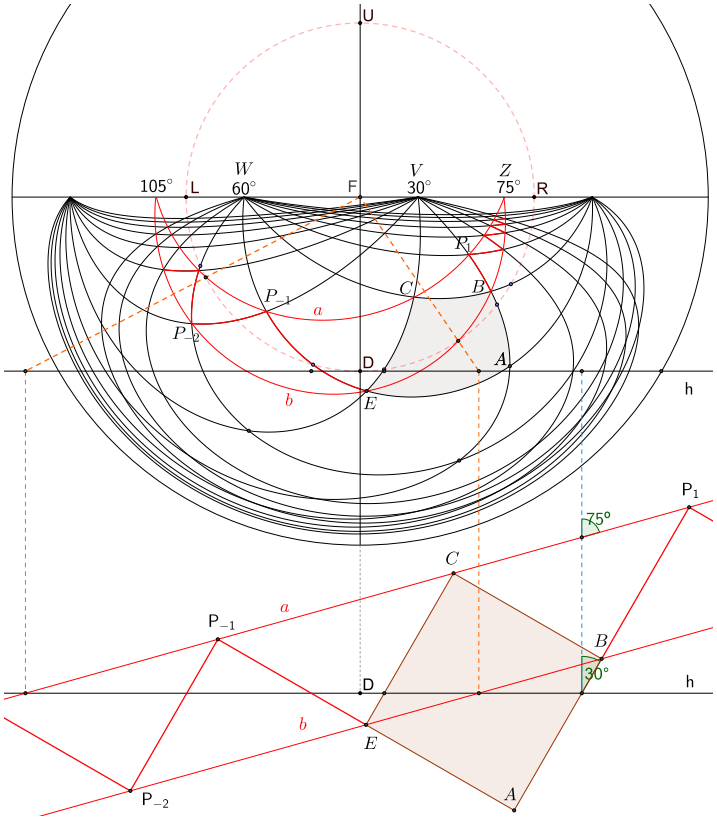

Fig. 20 Multiplication of a square to form a uniform grid, or floor tiling.

Dynamic Grids

Let us revisit grid methods. Using grids can be liberating, especially when drawing from nature, where ruler and compass constructions can become cumbersome. However, drawing on top of fixed grids like those of Figure 12 is also very limited. Most lines will not be in the class one chose to plot in the grid, and must be therefore guessed at with great uncertainty.

Araújo (2019b) proposes a method of that has the mechanical simplicity of a grid method without the limitations. The method works by exploiting the of a specific perspective to create a simple mechanical device that generates all geodesics from a . It can be implemented in other spherical perspectives (as we shall see ahead in the equirectangular case) that have other group symmetries. In the azimuthal equidistant case it works as follows: The LR-family of geodesics that cross the median plane at $\zeta \in [0, 90^\circ]$ (Figure 11) generates all others geodesics by rotation around the y-axis (that is, the **FB** axis), and that spatial rotation acts on the perspectrive plane as a rotation around F.

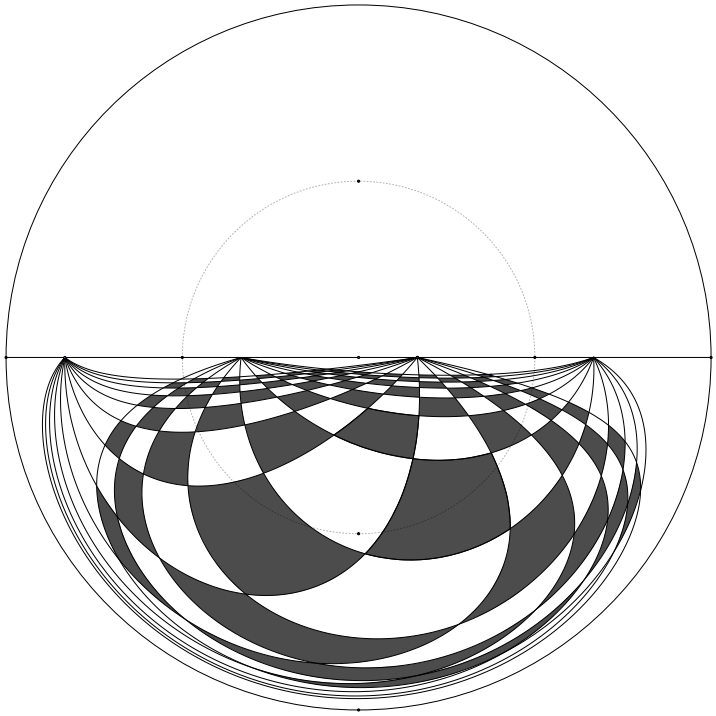

Fig. 21 The final uniform tiling, constructed in Figure 20.

Indeed, giving a geodesic is the same as giving a plane through O, and all planes through O will either be the coronal plane or intersect it on a diameter. The azimuth of the intersection, together with the dihedral angle ζ between the plane of the geodesic and the coronal plane therefore determines the geodesic. If we define the *apex* of the geodesic relative to $\overrightarrow{OF}$ to be the point of a geodesic that is closest to F, any geodesic outside the coronal plane is uniquely determined by the (θ_M, ζ_M) coordinates of its apex, with $\zeta_M \in [0, 90^\circ]$ and in $\theta \in [-180^\circ, 180^\circ]$. Then we can select a geodesic's ζ_M by picking one curve of the *LR* family and select the value of θ_M by rotating this chosen element around F, which changes θ_M for fixed ζ_M.

This suggests a simple mechanical method to draw the segment between two given point Araújo (2019b). Place a print of the *LR*-family of geodesics under a sheet of tracing paper, and fix one to the other by sticking a nail through point F in the print. The drawing will be executed on the tracing paper sheet. Then, given two points A and P drawn on the tracing paper sheet, rotate the drawing on top of the print; there is one and only one geodesic of the *LR* family that will pass through the given points. Once found, just trace over it. Of course, since we are only printing a finite number of geodesics, the correct geodesic will often be found between two printed ones, and can be traced by drawing between these, with a measurement error bounded by half the angular distance between printed lines.

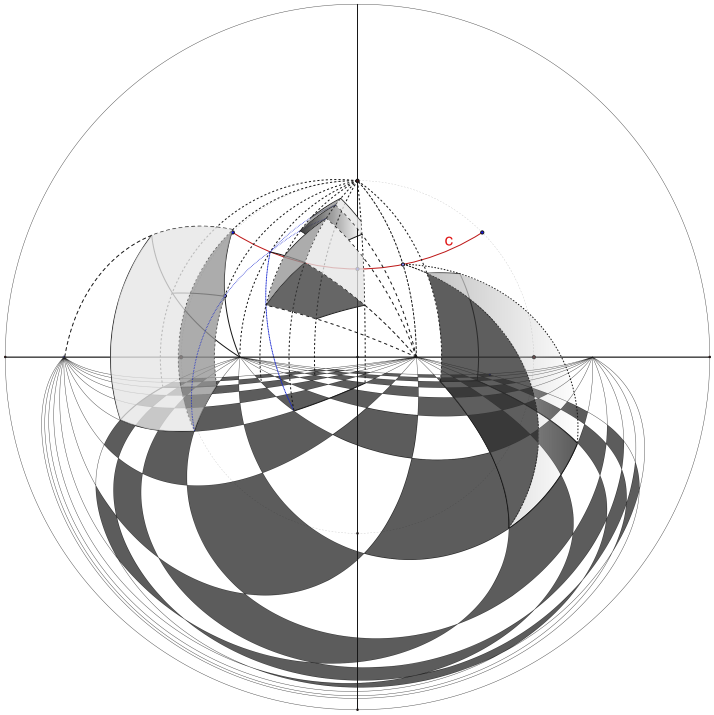

Fig. 22 Cubes and ramps, drawn using a ground tiling as reference and sending lines to vanishing points on the c, which is a circle of constant elevation 45°.

Unlike the ruler and compass methods of Barre and Flocon (1968) and Araújo (2018c) this method avoids the need for measuring and plotting special points in the construction of geodesics - any two points will do - and unlike the fixed grid methods it is not constrained by arbitrary setups. Also, when tracing from parametric plots we are using a more accurate rendering of geodesics (no longer using the arc of circle approximation), which may be somewhat more accurate when recovering the anamorphosis from the perspective (say, in VR renderings, which we will discuss ahead).

Drawing from Nature

We end the section with two drawings made from observation. The first one, a picture of a stairwell (Figure 24) drawn entirely with the ruler and compass methods, required careful measurements, and the preliminary construction of a plan and elevation of the scene. The steps of the stairs are built from line vanishing to F and U that bounce from twin sets of ramps going to common vanishing points at around 33° elevation.

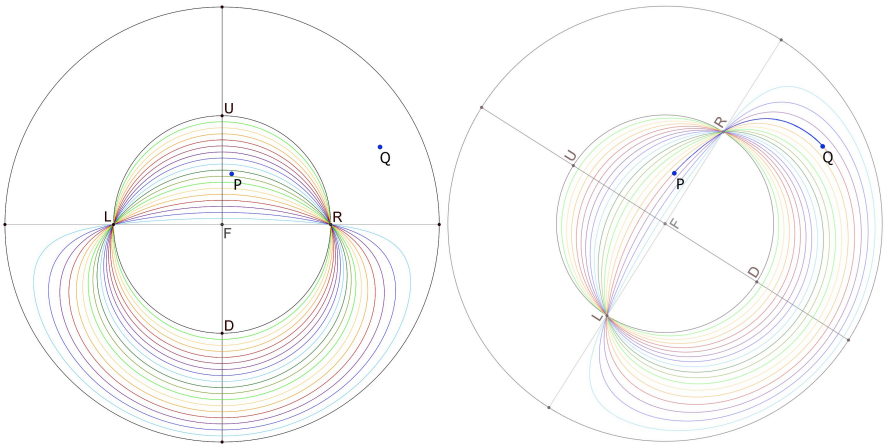

Fig. 23 Finding the geodesic that joins two given points A, B by rotation of the LR family around F. This can be executed mechanically by placing a tracing paper sheet over a print of the family of geodesics and sticking a pin through the center of both sheets. Then the tracing paper containing points A and B can be easily rotated around F while the printed geodesics remain fixed, and thus AB will be found.

The second example (Figure 25)) was sketched using the dynamic grid method in a much looser way, using a few key measurements to obtain the scene, which certainly is far from exact, and yet essentially correct. The two drawings are both small, fitting respectively into an A4 and an A3 drawing sheet, and show what can be done by an average draughtsman with the methods presented above.

Equirectangular Perspective

We will now consider a different flattening and its corresponding perspective: the . We will not go into as much detail as in the previous case, but rather establish parallels with it, while referring the reader to external references for details. Our point here is that there is a general schema, or strategy - although not an algorithm - for solving spherical perspectives. We will therefore stress the parallels between the two cases.

VR Panoramas as immersive anamorphoses

Before we start solving equirectangular perspective, lets us take the time to point out its peculiar connection with VR visualizations, for which it is particularly convenient.

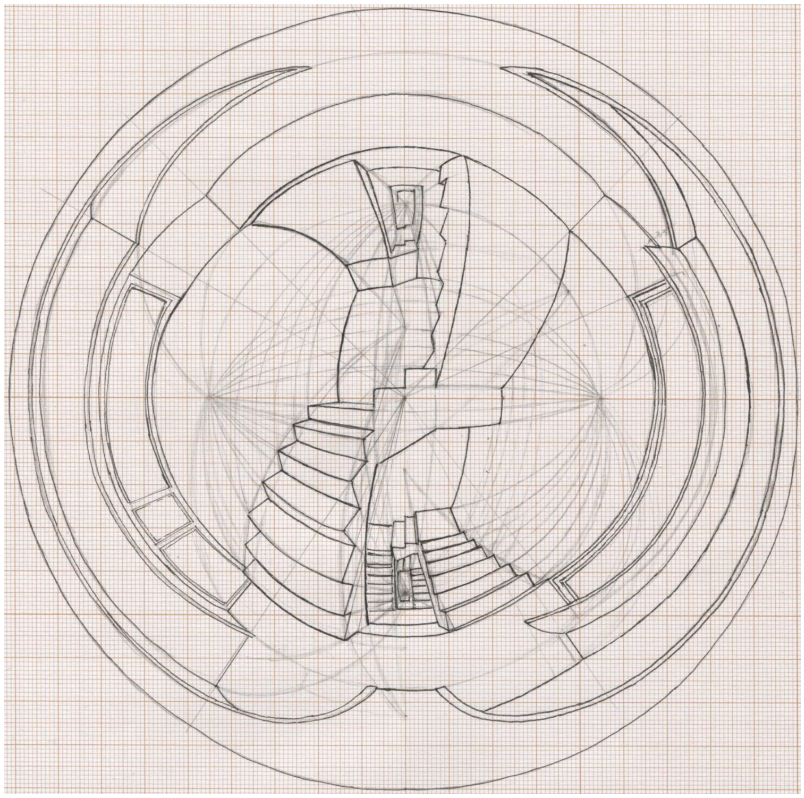

Fig. 24 Construction of a stairwell. Pencil and ink on graph paper. Drawing by the author.

As we have discussed above, spherical perspectives can be seen as repositories of the visual information of a spherical anamorphosis, that is, of an immersive optical illusion that elicits in the observer the impression of being surrounded by a 3D environment. The construction of immersive anamorphoses is a problem with a long history. The problem was posed and answered in various ways, from the partial to the fully immersive, and using a great variety of projection surfaces. Andrea Pozzo, among many, deals with this problem both theoretically (Pozzo 1693) and in his work itself (Fasolo and Mancini 2019), for anamorphoses on surfaces planar, multi-planar, or even irregularly curved. The hugely successful panoramas of the 19th century Grau (1999) dealt with the recovery of from , even if, as pointed out by Kemp (1990), these were usually not cylindrical at all but rather clever hacks involving the stitching of adequate linear perspectives (this is quite proper: the business of artists is to be clever magicians rather than mindful technicians). There were even attempts at spherical anamorphoses (Belisle 2015), although a spherical perspective as such was not yet formulated.

Most of these early anamorphoses required the creation of large scale architectonic structures wherein the *trompe l'oeil* could take form. Today we have a rather

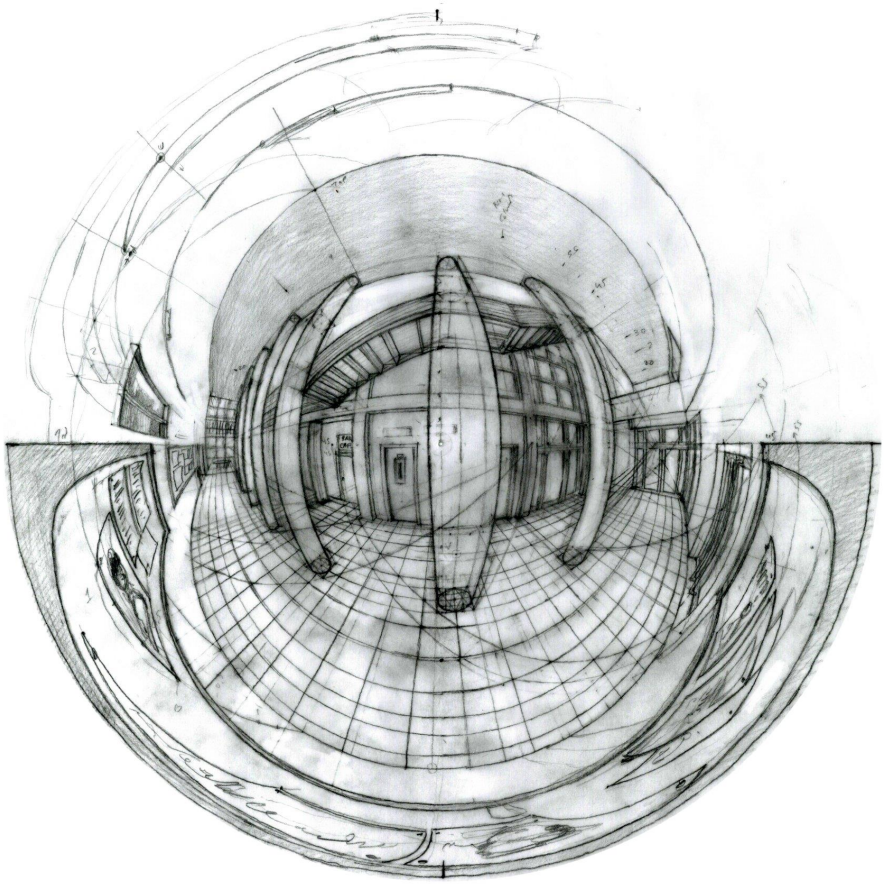

Fig. 25 Corridor and stairs. Pencil on paper. Drawing by the author.

more economic tool at our disposal, in the form of the . These panoramas work by taking an image file - usually photographic or a 3D graphics render - and wrapping it around a virtual sphere. Then a user may view them interactively by virtually pointing the screen (moving a mouse, or moving the head in a VR helmet), like a camera, at a desired section of the sphere. In terms of anamorphosis, the user controls the position of a rectangle in space, which defines a cone of rays that cuts the sphere, selecting a region of the spherical anamorphosis, and this rectangular anamorphosis is what is seen on screen (Figure 27). Risking pedantry, we point out that anamorphosis, being defined as an equivalence relation, is transitive, hence a (plane) anamorphosis of a (spherical) anamorphosis of a scene X is still an anamorphosis of X.

These panoramas have many applications in computer graphics; they can be used for environmental mapping or generally as painted backgrounds for 3D envi-

ronments (Greene 1986). Photographic (also called 360-degree photographs or VR photographs) created by image stitching have been extensively studied both in the methods of their accurate creation and of efficient interactive rendering (for a technical account see Benosman et al (2000)) and have many applications, from their uses in casual or artistic photography to scientific applications in the documentation cultural heritage sites Rossi (2017).

Our peculiar interest in these panoramas stems from the fact that we can use our handmade perspective drawings as source data for the same rendering engines that display VR photography. Indeed, the data files for these applications are constructed with the exact same chart projections that we use in our spherical perspectives.

Since, as we have discussed, all (total, compact) spherical perspectives are equivalent then we could, in theory, use any spherical perspective as source. In practice, VR engines are built to use certain specific formats, and we must either draw in the corresponding perspectives or use software to convert our drawings to them.

The common formats for VR panoramas are either cubical or equirectangular, the latter being the most common in photography applications. The azimuthal equidistant projection, unfortunately, is not common for these purposes. Although fisheye cameras naturally project light onto the sensor in a configuration that approaches the azimuthal equidistant projection, this is then converted to equirectangular format for further processing. Unlike the fisheye projection, which renders onto a disc, the equirectangular projection renders onto a 2×1 rectangle, thus fitting well with the rectangular nature of image files. The deformations of this projection are exhibited well by the equirectangular perspective drawing in Figure 26. They are similar to those of a cylindrical projection near the horizon and then become squarish as we approach the top and bottom edges of the picture. Since the drawing has been correctly drawn according to the precepts of equirectangular perspective (that we will discuss ahead) it can be loaded as is into any VR panorama engine which will render it as if it was a 360-degree photograph. In figures 28 and 29 we see two frames of such an interactive render, looking left and right along the corridor depicted in Figure 26. Note that in each linear perspective picture thus obtained, each line will exhibit at most one of the two vanishing points present in the full spherical perspective.

Note 7. Currently there are VR panorama visualizers freely available both in the desktop and in social media websites. The peculiarities of loading images into each such viewer (which sometimes involve metadata injections or image tagging) are ephemera better left to a quick online search, or to supplementary notes at the author's website (Araújo 2015).

We will now solve the equirectangular perspective by following the strategy we used in the azimuthal equidistant case: classify geodesics and their projections, then learn how to render them efficiently, with a focus on antipodal constructions. In this we will be following (Araújo 2018b).

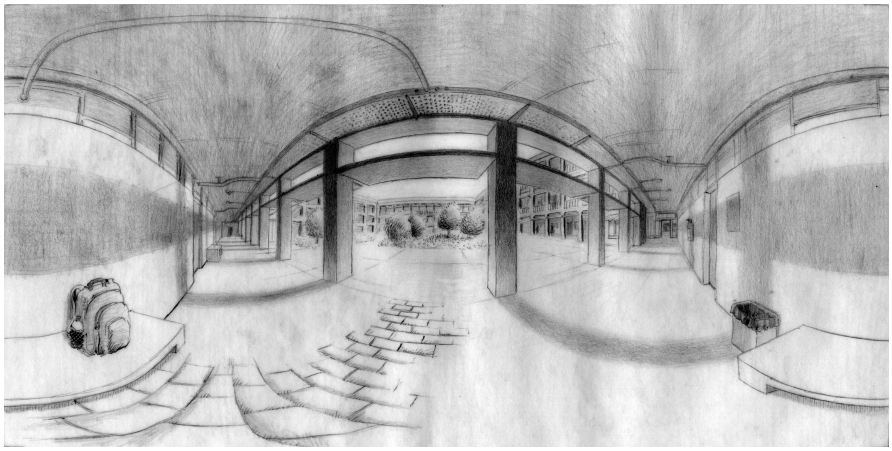

Fig. 26 An equirectangular perspective of a corridor and inner courtyard. Graphite on paper. Drawing by the author.

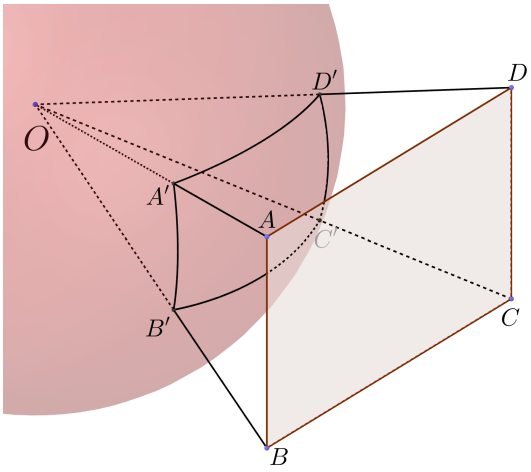

Fig. 27 An interactive Virtual Reality Panorma is obtained by projecting the spherical anamorphosis radially onto a rectangle that can move freely around O. Each such projection will capture at most one vanishing point of each line.

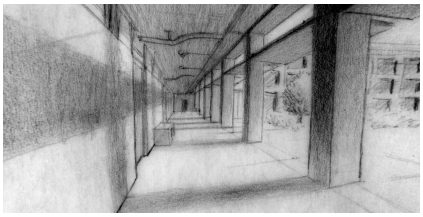

Fig. 28 Virtual Reality view of the panorama of Figure 26 (looking towards the left)

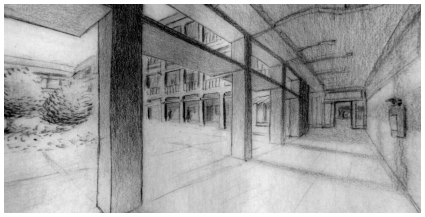

Fig. 29 Virtual Reality view of the panorama of Figure 26 (looking towards the right)

Construction of the equirectangular flattening

Equirectangular perspective is defined by the flattening of the same name. Again, this flattening is a well-known map projection; it was at one time attributed to Eratosthenes but present research tends to follow Ptolemy in crediting Marinus of Tyre (about A.D. 100) as its originator (Snyder 1993). The was very prevalent in maps due to the simplicity arising from their main property, that of transforming the graticules of the meridians and parallels (lines of constant longitude and latitude) into a uniform grid of verticals and horizontals on a projection rectangle.

We can construct this flattening in the following way: taking the same referential as in the previous sections we now release the meridians at points **U** and **D** and straighten them without stretching while keeping fixed the line of the horizon. This transforms the unit radius sphere into a cylinder of radius one and height π. Then we cut the cylinder vertically across **B** and unroll it onto the plane, as a rectangle of height π and length 2π, with F at the center. Lengths are preserved along the **UD** lines, which become verticals in the perspective rectangle. Both lengths and angles are also preserved along the line of the horizon. The map is a everywhere except at **U**, **D**, and at the **UBD** meridian. Points **U** and **D** become the top and bottom lines of the rectangle respectively (each point of the line representing a vector of the tangent plane) and **UBD** is sent to both the left and right borders of the perspective rectangle. Hence the border of the perspective rectangle is the blowup of this flattening, by definition 6.

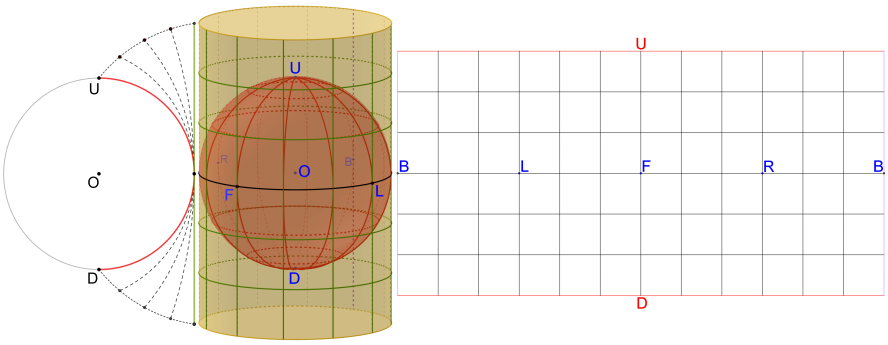

Fig. 30 Equirectangular flattening. Left: Straightening the **UD** meridians with horizon circle fixed transforms the unit sphere onto a cylinder of height π and radius one. Right: cutting the cylinder vertically through point **B** and unrolling it results in a 2×1 rectangle.

The flattening is very simple in terms of the horizontal coordinate system in equation 2 (recall also Figure 7). In terms of this system of coordinates a point **P** that projects on the sphere with bearing λ and elevation φ is projected onto the plane as the point $P = (\lambda, \varphi)$.

Images of geodesics

We must begin with a . Take once more the **LR** geodesics (Figure 10), as we did for the azimuthal equidistant case. If we plot them at 5 degree intervals with their maximum elevation φ_M in the interval $[0, 90°[$ we get the curves in Figure 33. It can be shown (Araújo 2018b) that these curves follow the equation

$$\varphi(\lambda) = \arctan(\tan(\varphi_M)\cos(\lambda)) \tag{4}$$

where φ_M is the angular elevation of the curve at its relative to $\overrightarrow{OU}$ (its point of maximum elevation), which in this case occurs for $\lambda_M = 0$, that is, on the median plane. When $\varphi_M = 90°$ the curves degenerate into the union of the two vertical lines, through *L* and *R*.

Analogously to the azimuthal equidistant case, we can obtain all other geodesic from the **LR** family by rotating it, but now around the $\overrightarrow{\mathbf{UD}}$ axis. The rotation determines the value of $\lambda_M \in]-180°, 180°]$ while the choice of geodesic in the family selects the value of $\varphi_M \in [0, 90°]$. Together they determine the apex and therefore the geodesic. The difference with regard to the azimuthal equidistant case is that this time the spatial rotation around the $\overrightarrow{\mathbf{UD}}$ by an angle δ acts as the translation $(\lambda, \varphi) \mapsto (\lambda + \delta, \varphi)$ in the perspective image. Hence the general geodesic is determined by the coordinates of the apex (λ_M, φ_M) in the form

$$\varphi(\lambda|\lambda_M, \varphi_M) = \arctan(\tan(\varphi_M)\cos(\lambda - \lambda_M)) \tag{5}$$

Ruler and compass approximations

The geodesic images in figure 33 may look somewhat daunting to the draughtsman at first. They turn out not to be so hard to draw in good approximation using a ruler, compass, and protractor. Modulo translational and reflection symmetries, the difficulty is reduced to the plot of the curves of the *LR* family in the interval $\lambda \in [-90°, 0°]$. What can we say about these?

A cursory look at the geodesic plot shows that the geodesic images are very similar to for . In fact, equirectangular drawings (26) look very similar to cylindrical perspectives for the regions of the image near to the horizon (the causal photographer may mistake an equirectangular photo for the photo panoramas of old, made by simply overlapping photos side by side on a wall). This cursory impression turns out to be partly accurate, but more can be said. As pointed out in Araújo (2018b):

1. For apex elevations smaller than $\varphi_M = 33°$ degrees a geodesic image is well approximated by the sinusoidal cuve that matches it at the apex and horizon. The maximum error is less than one degree for $\varphi_M < 29°$ and less than two degrees for $\varphi_M < 36°$. At $\varphi_M = 33°$ it equals $1.7°$.

2. As apex elevations grow larger than $\varphi_M = 33^\circ$, and just as the sinusoidal approximation breaks down, the geodesics become well approximated by the arcs of circle that match them at apex and horizon. At $\varphi_M = 33^\circ$ the circular approximation yields a maximum error of 1.6 degrees. This approximation holds well (maximum error under 2 degrees) until $\varphi_M = 60^\circ$, when the error is 1.9°.
3. When the apex rises above 60 degrees, the circular approximation becomes useless, as the geodesics assume their squarish from. Araújo (2018b) proposes a simple descriptive geometry construction that allows one to obtain points of the geodesic by using operations with ruler, compass and protractor. Even for an apex elevation as high as $\varphi_M = 80^\circ$ (see Figure 31), a mere four points thus calculated are enough to obtain an error of the order of 1 degree (using arc of circle interpolation in between the calculated points).
4. Because the equirectangular flattening preserves angles at the horizon, the perspective image of a geodesic whose apex has elevation φ_M makes an angle of φ_M with the perspective image of the horizon (see for instance the plot of the $\varphi_M = 80^\circ$ geodesic in Figure 31(right)). Since we also know that the tangent is flat at the apex, we have two tangents that can be used to constrain the drawing of the curve. These constraints are helpful with Bezier approximations.

We will not elaborate here on the construction mentioned on point 3 above. Details may be consulted in the work cited above. The point is that it puts equirectangular perspective on the list of perspectives that can be reasonably constructed without computers, even if it takes some effort. Having classified and rendered geodesics, we can now consider the line images within them.

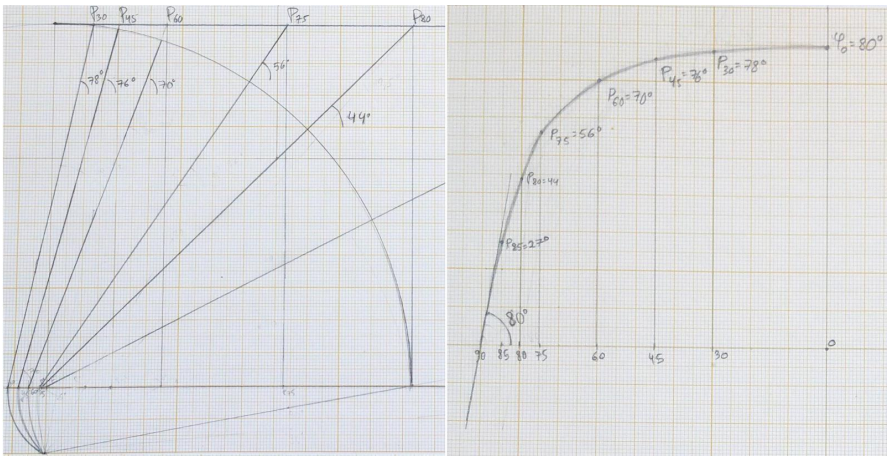

Fig. 31 A construction (left) of the $\varphi_M = 80^\circ$ geodesic (right) using a ruler, compass, and protractor, according to Araújo (2018b).

Drawing lines

Having understood the shape of the equirectangular geodesics, having learned how to plot them according to the coordinates of their apex by elementary means, we now need to learn how to plot lines themselves.

may take rather confusing, sigmoid shapes when seen in isolation. This confusion vanishes once we see them as meridians (halves) of geodesics. Then we know all of them are described by the curves of Figure 33 (modulo translation) by choosing a meridian between two vanishing points.

Note how we follow very much the same schema as in the azimuthal equidistant case:

First, we learn how to plot points from adequate angular measurements: this is easier in the present case, since equirectangular perspective relates very simply to the horizontal system, which is very natural to use in observations. Having measured the bearing λ and elevation φ of a point P (with a theodolite, from nature, or a protractor, from plans), the perspective image of P is just the point (λ, φ) in the perspective rectangle.

To find vanishing points of a line l, bring the line to O by translation to get line l_O, then plot the points of $l_O \cap S^2_O$.

We then learn how to plot antipodes: on the sphere you can get the antipode $P^\star$ of a point P by rotating 180 degrees around the z axis and then reflecting across the plane of the horizon. In the equirectangular flattening, the first operation becomes a translation of half the perspective rectangle's length and the second becomes a reflection across the line of the horizon.

Now we divide lines into classes, according to whether they intersect the horizon or not. The horizon takes, in this perspective, a role analogous to the corona's role in the azimuthal equidistant case.

Suppose a line does intersect the horizon. Measure the bearing λ_H at which this happens. If the line is on a vertical plane through O, then it projects into the union of two verticals, the one though $(\lambda_H, 0)$ and the one through its antipode, at a distance of 180 degrees along the horizon. Find a vanishing point V, plot this and $V^\star$. If these points are U and D, the line is vertical and projects as the vertical segment through $(\lambda_H, 0)$. If not, then the line contains either U or D. Find which, and project the meridian (consisting of two segments of the two lines) which contains U or D, according to the case.

If the line crosses the horizon but is not on a vertical plane through O, then it will fall on one of the LR geodesics modulo translation. Find where the line hits the horizon. Then the apex must be at 90 degrees from that point along the λ axis (find on which side by inspection). Having obtained λ_M, measure the elevation over that point to get the apex (λ_M, φ_M). Now just plot the proper geodesic, modulo translation by λ_M, as described in the previous section, and crop at the vanishing points.

If the line does not touch the plane of the horizon then it must have two vanishing points on it. Measure them in the usual way, then the bearing λ_M of the apex must

be halfway between them. Measure the elevation there to get the apex, and plot the geodesic, cropping at the vanishing points.

This briefly covers all cases. See Araújo (2018b) for more details.

The drawing of Figure 32 was done entirely with the methods just described. But ahead we will see how to use the symmetries of the perspective to avoid these auxiliary constructions in drawing practice.

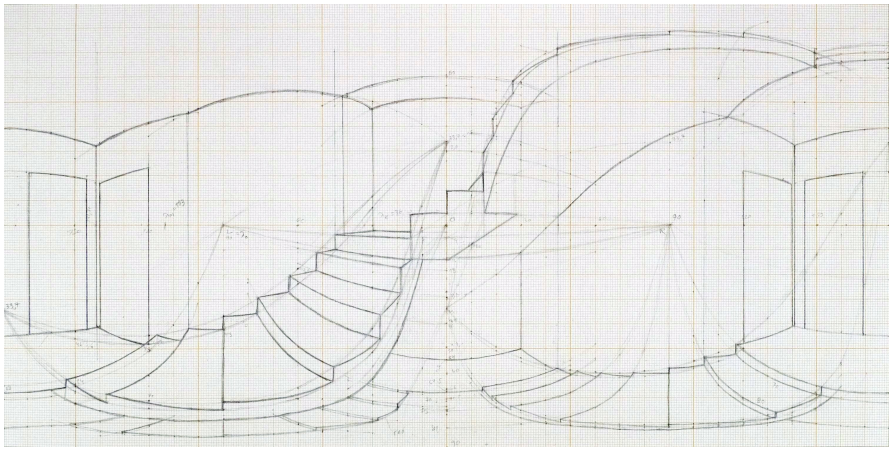

Fig. 32 The stairway of Figure 24, now in equirectangular perspective, constructed with ruler, compass and protractor. Graphite on graph paper. Drawing by the author. See author's website Araújo (2015) to view the corresponding VR panorama.

Sliding grids

The translational symmetry in equation 5 implies that, given the perspective images A, B of two spatial points, the geodesic segment image AB may be found by translating the LR family (Fig. 33) until a member of this family is found to go through A and B (see Figure 34). This may be exploited mechanically to make a very efficient "dynamical grid" sketching method (Araújo 2018a) analogous to the rotation grid method we described for the fisheye case: draw an equirectangular grid (or print one) onto a sheet of hard backed paper of a convenient size (say A4). Then take a sheet of tracing paper twice as large (A3 in this case), fold it in two to form an envelope of size A4, and place the print inside it. All the drawing is done on one side of the tracing paper envelope. When two points need to be joined, slide the print sideways along the fold of the tracing paper envelope, to implement mechanically the operation of Figure 34. After an adequate amount of sliding, a segment will be found to match both points. Trace it, and it is guaranteed that the curve obtained

is the correct projection of the segment **AB**. The maximum error will be half the separation of the printed geodesics.

This is of course analogous to the dynamic grid method we described for the azimuthal equidistant case, but now the mechanical device expresses the group of translations rather than rotations.

For convenience, the grid usually contains four copies of the *LR* family, one for each cardinal point, and another four, their reflections across the horizon (see Figure 35). Although this makes the grid more crowded, it helps the drawing process in some ways, since the physical print of the *LR* family, unlike the example of Figure 34 cannot flow cylindrically out of one edge to reappear at the opposite one (that is, physical translation is not translation modulo 360°). Therefore the repeated grid will avoid some awkward physical operations like grid inversions or the need to trace partial curves on opposite edges of the grid. In a digital process, of course, the grid can indeed flow cylindrically across opposite edges, and a sliding system has been implemented in the equirectangular drawing program *Eq A Sketch 360* (Araújo 2019a) which uses the much leaner system of Figure 34.

The simplicity of this operation hides its importance. It provides us with a practical and accurate , that is, it gives us a method to join any two points. The common practice among artists was until very recently to just trace over fixed grids, with all the limitations that entails, as most lines will not be in the grid. The analytic expression for the equirectangular line joining two given points of known coordinates seems too complex for ruler and compass construction (a derivation of this expression may be found in Araújo (2019a)). The ruler and compass method we described above is in fact a roundabout way of obtaining this line by relying on the measuring of special pairs of points that make the construction feasible; but the sliding grid method we just described reduces that computation to a simple, physical operation of visual inspection that can be performed with greater ease, and comparable precision, to ruler and compass constructions, for any two arbitrarily chosen points. This situation is in both its difficulties and their resolution quite similar to what we found in the azimuthal equidistant case.

The opens the way for easier drawing by *internal* perspective operations. In Figure 36 we see an example which comes from what is sometimes called the "" in classical perspective.

In the drawing, made from observation, only the proximal arch was measured from nature. Since it was know that the others had the same measurements, these were constructed by the following operations. Mark points *A* (upper left internal corner of the left column of the arch) and *B* (lower right external corner of the right column) as in the Figure. Then using the sliding grid method, draw the geodesic *AB*. Trace the vanishing set of the plane of the arches. In this case they are going left to right, so the vanishing set is the plane represented by the vertical line through point *R*. Where the geodesic *AB* intersects this line must lie the vanishing point of line *AB*, marked *B* in the figure. Now mark point *C* at the point of the second arch corresponding to point *A* of the first arch. Using the sliding grid method, trace line *CV*. Let *D* be the intersection of *CV* with the ground (that is, with line *BR*). Since the arches are congruent, then the diagonals *AB* and *CD* are parallel, hence *D* must

be the point of the second arch that corresponds to B on the first. We have obtained the second arch. Repeat as needed to get the rest.

There are many such operations from classical perspective that translate easily once we have a spherical perspective straightedge. Many such operations in fact work better in spherical perspective, since compactness ensures that all the vanishing points will be available inside the drawing paper.

Spherical straightedges in digital drawing programs

We have seen the importance of a spherical straightedge for internal perspective constructions, and how this straightedge is made available for handmade spherical perspective drawings. Of course in the digital realm such a straightedge can be obtained with greater ease and precision.

In (Araújo 2019a) an analytic expression is derived for the geodesic that goes that goes through two arbitrary points. This was then used for programming a digital equirectangular straightedge - a snapping system for drawing geodesics - in the drawing application . This is a piece of free, experimental software for teaching and drawing equirectangular perspective. As of this writing, *Eq A Sketch 360* (available at Araújo (2015)) seems to be the only drawing program to implement both a sliding grid and an equirectangular straightedge that works as a : the user selects two points on the screen and the drawing pen or mouse snaps to the geodesic AB, that is, draws only over the path of the geodesic.The sliding grid is used in combination with the snapping system as a measuring device to plan the perspective constructions.

In its latest version (september 2020), the Microsoft Garage app *Sketch 360* has now adopted a sliding grid into its set of tools, though not yet a snapping system for general geodesics.

Note 8. For the azimuthal equidistant case there exists a vectorial drawing program implemented as a script in (available at the author's website Araújo (2015)) that draws arbitrary geodesics, but currently no raster drawing app. The calculations required for programming the azimuthal equidistant case are an adaptation of those described in Araújo (2019a) for the equirectangular case.

Final reflections: what is (not) a spherical perspective

We have been concerned with defining what a spherical perspective is. It is just as enlightening to consider what it is not. Definitions, of course, are just ways of organizing concepts, and they are quite arbitrary, but we need to at least settle momentarily upon on a working meaning for our terms if we are not to get hopelessly lost. This has been the case for long with the term "", as well as its relative, "", both heavily loaded terms that have been often discussed without any definition being at-

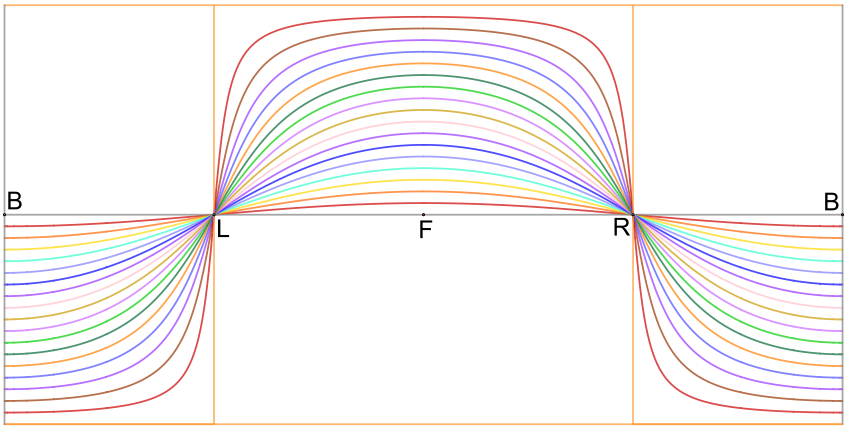

Fig. 33 Equirectangular projection of the LR family of geodesics at 5-degree intervals of maximum elevation.

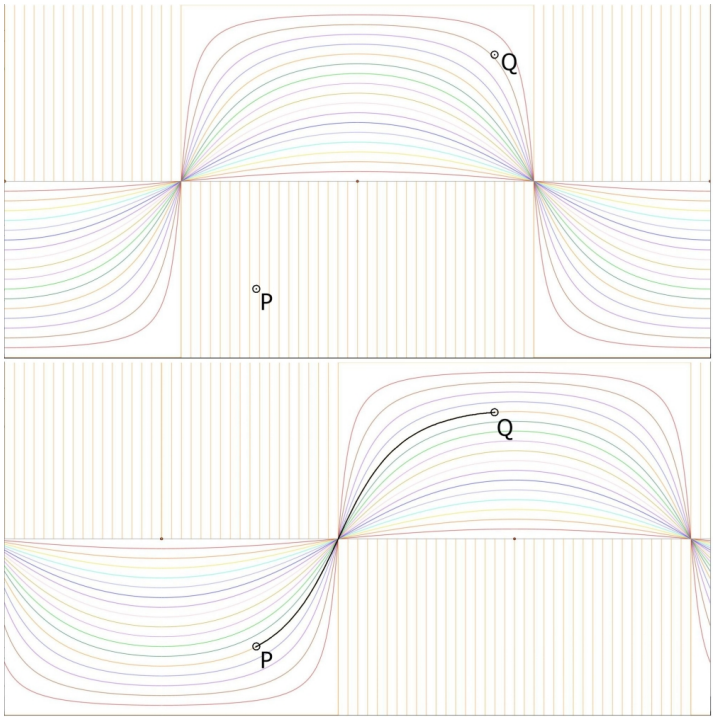

Fig. 34 Sliding the *LR* family of geodesics to find the geodesic segment that joins points *A* and *B*. Drawn with the free software Eq A Sketch 360 (Araújo 2019a). Additional verticals are marked for measuring convenience.

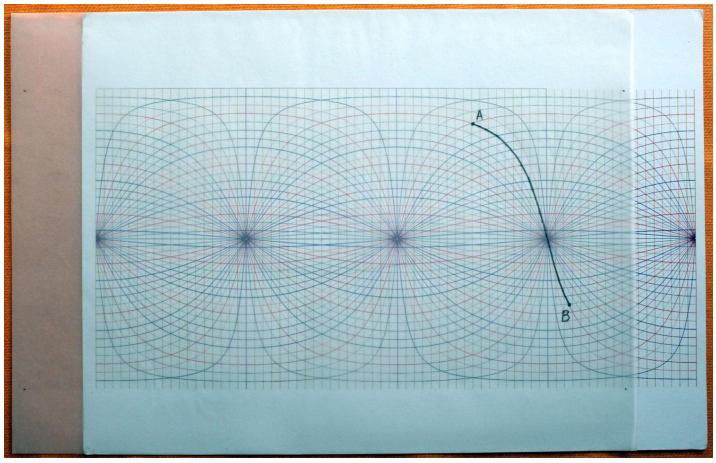

Fig. 35 Equirectangular grid, with copies of the *LR* family centered on each cardinal point and reflected over the horizon for convenience. Verticals are also marked at 5 degree intervals. The grid is sliding inside a tracing paper envelope where the drawing is done. In the figure, it slid about 40 degrees to the right to find the line joining *A* and *B*.

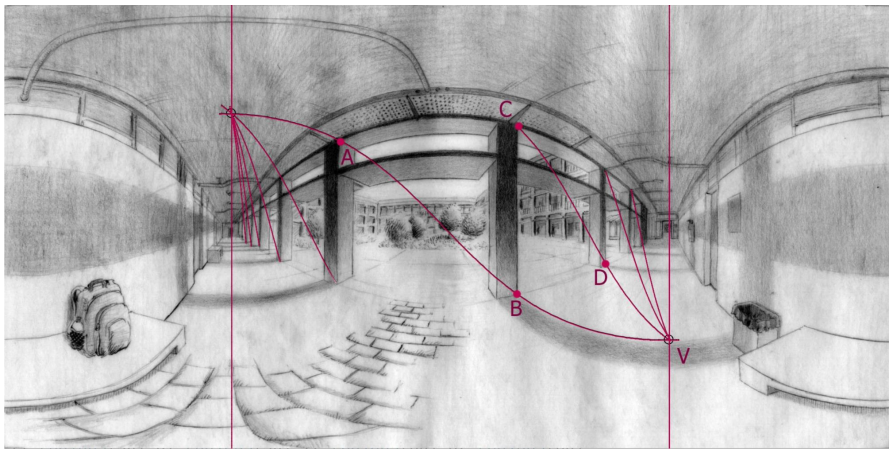

Fig. 36 Telephone pole problem. The arch delimited by *A* and *B* was measured from observation. Once drawn, it was used as a template to construct the other arches by internal operations. See author's website Araújo (2015) to view the corresponding VR panorama.

tempted leading to endless confusion in theory, artistic practice, and historical study (Andersen 2007, p. 109).

To gain some clarity, we have followed here the definition of (Araújo 2018c) (slightly adapted). We may want to stop and consider what it encompasses and what it doesn't.

The technical definition 5 is somewhat heavy, so let us recall its intuitive meaning: from a 3D scene, projected radially on a sphere and then made compact by

adding vanishing points, we get a spherical anamorphosis. A is the flattening of that , that is, the mapping of the anamorphosis onto a compact region of the plane, following certain conditions of continuity.

This definition includes the things that have traditionally been called by the term ”spherical perspective”. It includes the azimuthal equidistant and equirectangular case. These are *total* spherical perspectives, in the sense that they project the whole sphere.

We can trivially expand definition 5 to cover what we called *partial* spherical perspectives in note 3, and then the definition covers Barre and Flocon's perspective, being the restriction of the azimuthal equidistant perspective to a single hemisphere. It also covers cylindrical perspective and most things that have been traditionally called ”curvilinear perspectives”, a vague term that we don't attempt to define formally here, as we don't really need it.

Our definition of spherical perspective insists on , and that leads us to our main, perhaps surprising exclusion: our definition does not cover classical perspective. To be sure, it covers any actually constructible linear perspective drawing! The restriction of linear perspective to any compact region, like a rectangle *is* a spherical perspective, and the rectangle can be as large as you want. It just cannot be the whole plane, which is not compact. And we cannot get the projective plane by our schema, since we don't identify opposite directions. We split them quite deliberately: we want a line to have *two* vanishing points in a total spherical perspective, not one. Hence, even as we open a spherical anamorphosis up to a hemisphere, so that the rays cover a whole plane, we find that frontal lines will have two vanishing points. This may be seen already at the edge of Barre and Flocon's perspective. By contrast, in the , we would be finding all lines to have one vanishing point. Ours is a fundamentally different construct, and we have already discussed why we think it is, for our purposes, the right one.

We could of course drop compactness and reasonably call the result a non-compact spherical perspective. Then we could allow classical perspective, and we could allow the use stereographic projections in a total perspective, as well as many other useful and interesting projections. But here we have focused on the compact ones because we think these bring something elegant into focus, which merits special attention: having all vanishing point accessible for effective drawing constructions, and allowing the full reconstruction of the immersive anamorphosis from the flat perspective drawing.

Even if they are a restricted set, compact spherical perspectives cover many things, some not obvious at first sight. For instance Correia and Romão (2007) proposes a computational Extended Perspective System, with applications to architecture (Correia et al 2013), which encompasses cylindrical, hemispherical perspective, and linear perspective, among others. It does this by changing the surface of projection smoothly according to some parameter (radius, eccentricity) to change, for instance, a cylinder into a rectangle, or a half sphere into a half-ellipsoid continuously. This in turn will change the plane projection smoothly. This may seem different from our perspectives, since we always start from a spherical anamorphosis. Yet, these are still *conical* anamorphoses and as we have discussed, spherical

anamorphosis is the canonical conical anamorphosis. It can represent any other. If you project radially onto a cylinder or an ellipsoid, or any starred surface, you are still getting, in the end, a (partial or total) spherical perspective. Then any transformation of the projection surface (say, from a sphere to an ellipsoid) results in a change of the final perspective image that can be equally accomplished by an adequate change of the sphere's flattening map.

This is not to say that the use of different surfaces is irrelevant. It is not. It may often be much more intuitive to think of a change of the flattening in terms of a change of projection surface. What we are saying is that these perspectives are encompassed by the present definition (whether they result in perspectives amenable to handmade drawing is a different matter).

This same argument shows that cubical perspective is also a spherical perspective in our sense. Recall that a is an image obtained by projecting a 3D scene radially onto a cube, then cutting open the cube and flattening it Rossi et al (2018). This projection, which recalls the tradition of perspective boxes (Verweij 2010; Spencer 2018), has now many uses in computer graphics (Greene 1986). It can be treated as a perspective, in the general sense of the word, by simply seeing it as an organized set of six linear perspectives (see for instance Olivero et al (2019a)). But is can also be seen, much more elegantly, as a spherical perspective. Again, the fact that the projection is made onto a cube is irrelevant. The cube is homeomorphic to the sphere by a radial map, so, for our purposes, a cube might as well be a sphere. We take the radial projection of the sphere onto the cube as the first step of the flattening, and the usual planification of the cube as the second step. Cubical perspective can then be treated according to our general strategy above: we can talk of geodesics on the cube, of antipodes, of line classification and rendering, in a way that is far more efficient and elegant than seeing it simply as a group of six somehow related classical perspectives. This has been done in (Araújo et al 2020), following very much the same approach we used here for the two cases we treated explicitly. It would be interesting to try the same approach on other polytope-based perspectives, such as the tetraconic perspective of Adams (1976).

All of these perspectives (cylindrical, cubical, etc.) are encompassed in our definition for the simple reason that they are conical, that is, they satisfy radial occlusion. So our spherical perspectives are not only compact, but fundamentally conical. If we overvalued accuracy over terseness we might have named this chapter quite correctly as *conical, compact, total* spherical perspectives. What if we dropped radial occlusion? We could certainly project onto the sphere in a non-radial way, and then obtain flattenings of that. Should we include these perspectives as "spherical"? Spherical non-conical? We could, but it is a delicate choice, as a concept loses interest if it encompasses too much. So we elect not to. As an example of what is left out, consider spherical reflections.

is a time honoured way of drawing a wide angle view without need for formal dominion of the projection (see for instance Jan Van Eyck's *Portrait of John Arnolfini and his Wife* (1434)). The artist can simply look at a spherical mirror and draw what he sees. The canonical example in the modern mind is Escher's *Hand with Reflecting Sphere* (1935). The end result is very similar in aspect to a fisheye perspective.

Yet, on careful analysis, it is fundamentally different, because occlusion is *not* radial. The points that occlude each other in a sphere reflection are not aligned atop rays that stem from a central point in the observer's eye. Hence, although Escher's famous print looks very much like a fisheye drawing, it is fundamentally different: the set of points represented is simply not the same, even when the angle covered is. The set of equivalent points in the reflected image does not respect the principle of radial occlusion. Since the picture does not derive from a conical anamorphosis, it cannot be represented as a spherical perspective in our sense of the word, since the anamorphic step is broken. For more on sphere reflections and their relations with perspective see Crannell (2011); Glaeser (1999); Araújo (2018c).

Reflections are just the most obvious of the things we are leaving out of our definition and that could conceivably be called perspectives, or even spherical perspectives.

Definitions are tentative, but they are crucial to help us delimit, separate, classify, and clarify. It is useful that we have a clear way of separating very similar looking things; to express clearly why Escher's reflection sphere and a fisheye picture are fundamentally different. A sphere reflection may define a curvilinear perspective, maybe even a spherical perspective if you so decide to define it so, but certainly not a total, conical, compact, spherical perspective.

These partitions of concepts are not just nitpicking. They have technical implications, in computing for instance: the fact that our perspectives are conical, means that occlusion computations are completely determined at the anamorphosis step, and in the exact same way for any spherical perspective. We two steps are computationally separate, and functionally composable. Further, occlusion being radial implies that we can use the same hidden faces algorithms as in classical perspective! This is not the case at all with reflections, where computing occlusion is a far more complex task (Glaeser 1999).

Even within the realm of our very specifically restricted spherical perspectives (total, conical, compact), we have available a large variety of image creating structures, each of which opens new aesthetic avenues for the artist, problems for the geometer, and opportunities for the technologist. We believe that the tools here presented may can help both the artist and the geometer to tame the curious members of this perspective bestiary. And, outside the realm of these spherical perspectives there are a infinite varieties of other "perspectives" yet to classify and put to use. Hopefully this chapter has also shaped a vague glimpse of this further realm in the reader's mind.

Cross-References

Anamorphosis Reformed: from Optical Illusions to Immersive Perspectives

References

Adams KR (1976) Tetraconic Perspective for a Complete Sphere of Vision. Leonardo 9(4):289–291, DOI 10.2307/1573354

Adams KR (1983) Flat Sphere and Tetraconic Perspective (Letter to Ed.). Leonardo 16(4):333

Andersen K (1992) Brook Taylor's Role in the History of Linear Perspective. In: Brook Taylor's Work on Linear Perspective, Springer, New York, pp 1–67

Andersen K (2007) The Geometry of an Art: The History of the Mathematical Theory of Perspective from Alberti to Monge. Springer Science & Business Media, New York

Araújo A (2017) Anamorphosis: Optical Games with Perspective's Playful Parent. In: Silva JN (ed) Proceedings of the Recreational Mathematics Colloquium V (2017) - G4G Europe, Associação Ludus, Lisbon, pp 71–86

Araújo A (2018a) Let's Sketch in 360º: Spherical Perspectives for Virtual Reality Panoramas. In: Bridges 2018 Conference Proceedings, Tessellations Publishing, pp 637–644

Araújo AB (2015) Notes on Spherical Perspective. http://www.univ-ab.pt/~aaraujo/full360.html

Araújo AB (2016) Topologia, anamorfose, e o bestiário das perspectivas curvilíneas. Convocarte–Revista de Ciências da Arte (2):51–69

Araújo AB (2018b) Drawing equirectangular VR panoramas with ruler, compass, and protractor. Journal of Science and Technology of the Arts 10(1):2–15, DOI 10.7559/citarj.v10i1.471

Araújo AB (2018c) Ruler, compass, and nail: Constructing a total spherical perspective. Journal of Mathematics and the Arts 12(2-3):144–169, DOI 10.1080/17513472.2018.1469378

Araújo AB (2019a) Eq A Sketch 360, a Serious Toy for Drawing Equirectangular Spherical Perspectives. In: Proceedings of the 9th International Conference on Digital and Interactive Arts, ACM, Braga Portugal, pp 1–8, DOI 10.1145/3359852.3359893

Araújo AB (2019b) A fisheye gyrograph: Taking spherical perspective for a spin. In: Goldstine S, McKenna D, Fenyvesi K (eds) Proceedings of Bridges 2019: Mathematics, Art, Music, Architecture, Education, Culture, Tessellations Publishing, Phoenix, Arizona, pp 659–664, available online at http://archive.bridgesmathart.org/2019/bridges2019-659.pdf

Araújo AB (2020) Explorations in Rational Drawing. Journal of Mathematics and the Arts 14(1-2):4–7, DOI 10.1080/17513472.2020.1734437

Araújo AB, Olivero LF, Antinozzi S (2019) HIMmaterial: Exploring new hybrid media for immersive drawing and collage. In: Proceedings of the 9th International Conference on Digital and Interactive Arts, ACM, Braga Portugal, pp 1–4, DOI 10.1145/3359852.3359950

Araújo AB, Olivero LF, Rossi A (2020) A Descriptive Geometry Construction of VR panoramas in Cubical Spherical Perspective. diségno (6):35–46, DOI 10.26375/disegno.6.2020.06

Barnard ST (1983) Interpreting perspective images. Artificial intelligence 21(4):435–462

Barre A, Flocon A (1968) La Perspective Curviligne. Flammarion, Paris

Barre A, Flocon A (1987) Curvilinear Perspective: From Visual Space to the Constructed Image. University of California Press

Barre A, Flocon A, Bouligand G (1964) 'Etude comparée de différentes méthodes de perspective, une perspective curviligne. Bulletin de la Classe des Sciences de La Académie Royale de Belgique 5(L)

Belisle B (2015) Nature at a glance: Immersive maps from panoramic to digital. Early Popular Visual Culture 13(4):313–335

Benosman R, Kang S, Faugeras O (2000) Panoramic Vision. Springer Verlag, New York

Berggren JL (1981) AI-Biruni on Plane Maps of the Sphere. Journal for the History of Arabic Science (5):191–222

Brownson CD (1981) Euclid's optics and its compatibility with linear perspective. Archive for history of Exact Sciences pp 165–194

Burton HE (1945) Euclid's optics. Journal of the Optical Society 35(5):357–72

Casas F (1983) Flat-Sphere Perspective. Leonardo 16(1):1–9, DOI 10.2307/1575034

Casas F (1984) Polar Perspective: A Graphical System for Creating Two-Dimensional Images Representing a World of Four Dimensions. Leonardo 17(3):188–194, DOI 10.2307/1575189

Catalano G (1986) Prospettiva Sferica. Università degli Studi di Palermo, Palermo
Correia JV, Romão L, Ganhão SR, da Costa MC, Guerreiro AS, Henriques DP, Garcia S, Albuquerque C, Carmo MB, Cláudio AP, Chambel T, Burgess R, Marques C (2013) A New Extended Perspective System for Architectural Drawings. In: Zhang J, Sun C (eds) Global Design and Local Materialization, vol 369, Springer Berlin Heidelberg, Berlin, Heidelberg, pp 63–75, DOI 10.1007/978-3-642-38974-0_6
Correia V, Romão L (2007) Extended perspective system. In: Proceedings of the 25th eCAADe International Conference, pp 185–192
Crannell A (2011) Perspective drawings of reflective spheres. Journal of Mathematics and the Arts 5(2):71–85
de Smit B, Lenstra Jr HW (2003) The Mathematical Structure of Escher's Print Gallery. Notices of the AMS 50(4):446–451
Escher MC (1956) Print Gallery. Litograph
Fasolo M, Mancini MF (2019) The 'Architectural' Projects for the Church of St. Ignatius by Andrea Pozzo. diségno (4):79–90, DOI 10.26375/disegno.4.2019.09
Glaeser G (1999) Reflections on spheres and cylinders of revolution. Journal for Geometry and Graphics 3(2):121–139
Grau O (1999) Into the Belly of the Image: Historical Aspects of Virtual Reality. Leonardo 32(5):365–371, DOI 10.1162/002409499553587
Greene N (1986) Environment mapping and other applications of world projections. IEEE Computer Graphics and Applications 6(11):21–29
Hohenwarter M, Borcherds M, Ancsin G, Bencze B, Blossier M, Delobelle A, Denizet C, Éliás J, Fekete Á, Gál L, Konečný Z, Kovács Z, Lizelfelner S, Parisse B, Sturr G (2013) GeoGebra 4.4. Http://www.geogebra.org
Kemp M (1990) The Science of Art. Yale University Press, New Haven and London
Michel G (2013) 'L'oeil, au Centre de la Sphere Visuelle. Boletim da Aproged (30):3–14
Michel G (n.d.) Dessin à main levée du Cinéma Sauveniére. http://autrepointdevue.com/blog/wp-content/vv/vv-gm-sauveniere/vv-gm-sauveniere.html
Moose M (1986) Guidelines for Constructing a Fisheye Perspective. Leonardo 19(1):61–64
Olivero LF, Rossi A, Barba S (2019a) A Codification of the Cubic Projection to Generate Immersive Models. diségno (4):53–63, DOI 10.26375/disegno.4.2019.07
Olivero LF, Sucurado B, Olivero LF, Sucurado B (2019b) Analogical immersion: Discovering spherical sketches between subjectivity and objectivity. Estoa Revista de la Facultad de Arquitectura y Urbanismo de la Universidad de Cuenca 8(16):80–109, DOI 10.18537/est.v008.n016.a04
Pozzo A (1693) Perspectiva Pictorum et Architectorum. Rome
Rossi A (2017) Immersive High Resolution Photographs for Cultural Heritage, vol 2. libreriauniversitaria.it, Padova
Rossi A, Olivero LF, Barba S (2018) "CubeME", a variation for an immaterial rebuilding. In: RAPPRESENTAZIONE/MATERIALE/IMMATERIALE Drawing as (in) Tangible Representation, Cangemi Editore, pp 31–36
Savage-Smith E (2015) Celestial Mapping. In: Harley J, Woodward D, Lewis G (eds) The History of Cartography, University of Chicago Press, pp 12–70
Schofield W, Breach M (2007) Engineering Surveying, Sixth Edition, 6th edn. Butterworth-Heinemann, Amsterdam ; Boston
Snyder JPP (1993) Flattening the Earth: Two Thousand Years of Map Projections. University of Chicago Press
Spencer J (2018) Illusion as ingenuity: Dutch perspective boxes in the Royal Danish Kunstkammer's 'Perspective Chamber'. Journal of the History of Collections 30(2):187–201
Termes D (1998) New Perspective Systems. self-published
Termes DA (1991) Six-point perspective on the sphere: The termesphere. Leonardo 24(3):289–292
Verweij A (2010) Perspective in a box. In: Architecture, Mathematics and Perspective, Springer, pp 47–62